2009

Flow Visualization In Microfluidic Expansion And Mixing

Ehsan Yakhshi-Tafti
University of Central Florida, ehsan.yt@gmail.com

FLOW VISUALIZATION IN MICROFLUIDIC EXPANSION AND MIXING

by

EHSAN YAKHSHI-TAFTI
M.S. Amirkabir University of Technology (Tehran Polytechnique, Iran), 2005

A thesis submitted in partial fulfillment of the requirements
for the degree of Master of Science
in the Department of Mechanical Engineering
in the College of Engineering and Computer Science
at the University of Central Florida
Orlando, Florida

Summer Term
2009

Major Professors: Ranganathan Kumar and Hyoung. J. Cho

ABSTRACT

Micro particle image velocimetry (μPIV) is a non-intrusive tool for visualizing flow in micron-scale conduits. Using this investigative instrument, two experimental studies were performed to understand flow behaviors in microfluidic channels - a sudden expansion step flow and laminar velocity profile variation in diffusion driven mixing. First, flow in a backward facing step feature (1:5 expansion ratio) in a microchannel was taken as the subject of μPIV flow visualization. The onset and development of a recirculation flow was studied as a function of flow rate. This flow pattern was further used to investigate two major parameters affecting μPIV measurements; the *depth-of-focus* and recording *time-intervals* between images in a μPIV image pair. The onset of recirculation was initiated at flow rates that correspond to Reynolds numbers, Re>95, which is well beyond the typical working range of microfluidic devices (Re=0.01-10). The recirculation flow has a 3D structure due to the dimensions of the microchannel and the effect of no slip condition on the walls. Ensemble cross-correlation was found not to be sensitive to variations of depth-of-focus and the output flow fields were similar as long as the overall optical focus remained within the upper and lower bounds of the microchannel. However, variations of time intervals between images in a μPIV pair, resulted in quantitatively and qualitatively different flow patterns for a given constant flow rate and depth-of-focus. In the second experiment, the effect of the laminar velocity profile and its variation on mixing phenomena at the reduced scale is studied. It is shown that the diffusive mass flux between two miscible streams, flowing in a laminar regime in a microchannel, is enhanced if the velocity at their diffusion interface is increased. Based on this idea, an in-

plane passive micromixing concept is proposed and implemented in a working device (sigma micromixer). This mixer shows considerable mixing performance by periodically varying the flow velocity profile, such that the maximum of the profile coincides with the transversely progressing diffusion fronts repeatedly throughout the mixing channel. μPIV has been used to visualize the behavior of laminar flow inside the micromixer device and to confirm the periodic variation of the velocity profile through the mixing channel.

To *Ghazal* and *Nili*

And *Mahnaz* and *Jafar*

TABLE OF CONTENTS

LIST OF FIGURES

INTRODUCTION

Microfluidics research and technology is an emerging interdisciplinary field developed at the intersection of chemistry, life sciences and physics (mainly fluid mechanics). Microfluidics involves study of the behavior of fluids flowing in very small conduits, typically at micrometer scales. Microfluidic devices and applications often involve minute volumes of fluid and transport processes which are dominated by molecular diffusion and not inertial effects. As the length of a system is scaled down, surface (L^2) to volume (L^3) ratio in a system increases indicating that surface and interfacial effects gain more significance compared to body forces such as inertia. For example a ten fold decrease in the characteristic length will reduce the surface 100 fold, and the volume to get smaller 1000 times; however the surface to volume ratio would increase 10 fold compared to the original ratio. The behavior of fluids at the reduced scale is highly influenced by factors such as surface tension, energy dissipation, quick thermal relaxation and fluidic resistance. By scaling down a system many new applications have been explored, in spite of challenges and shortcomings in actual realization of such systems. For example, fluids flowing side-by-side, do not necessarily mix in the traditional sense; molecular transport between them must often be through diffusion, a relatively slow process.

Fundamental science regarding fluid flow at reduced scales as well as applied technology targeted toward use in biochemical analytical systems are topics of ongoing research. Study of slip conditions on surfaces for gas and liquid flows (Lockerby, Reese et al.

2004; Lauga, Brenner et al. 2007), effects of miniaturizing on emulsions and surfactant functionality (Thorsen, Roberts et al. 2001), breakup of nano-jets (Moseler and Landman 2000), multiphase (liquid/liquid and liquid/gas) micro-flows (Stone, Stroock et al. 2004), anomalous diffusion (Basu, Wolgemuth et al. 2004), hydrodynamic dispersion and diffusion in non-newtonian systems (Daniel 2001) boiling regimes in microchannels (Kandlikar 2002), microsystems with chaotic flow (Yi-Kuen, Deval et al. 2001) and adsorption (physical/chemical) phenomena (Huber, Manginell et al. 2003) are some of the active areas of fundamental research using microfluidic devices and concepts. Development of inkjet printers, DNA sequencing chips, lab-on-a-chip technology and thermal microdevices are some examples of applied microfluidics.

Flow visualization has been essential to the development of the field of microfluidics. As the name *microfluidics* implies, the channels and conduits that contain the flows are extremely small and insertion of any kind of probes into the devices for flow measurement is usually impractical. Non-invasive flow visualization is important for the fundamental understanding of the nature of micro-flows, analysis and development of novel microfluidic devices, study of the related phenomena and providing data for validation of computer aided simulation results (Sinton 2004). Particle-based visualization techniques have been widely practiced in the field of microfluidics and involve dispersion of tracking particles in the fluids. These particles can follow the fluid reasonable well and velocity of fluids is inferred from recording the motion of the particles. Laser Doppler Anemometry (LDA) Particle Image Velocimetry (PIV) and Particle Streak Velocimetry (PSV) are major particle-based techniques that are used for

non-invasive flow visualization. In LDA, illumination from two laser sources form an optical interference intersection; passage of highly reflective tracking particles through the illumination volume causes shifts in the interference fringes. Displacement of the fringes divided by time gives the velocity of fluid at the illumination spot. This method is mostly used for macro scale applications as a number of complications arise when length scales are reduced (Tieu, Mackenzie et al. 1995). In PSV, streaks of particles (e.g. fluorescent dye) are tracked over a period of time on a single image. This technique has very low resolution and only provides sparse information for the velocity field but requires less experimental infrastructure (Brody, Yager et al. 1996). In PIV, the flow domain is illuminated by generating a two dimensional light sheet (macro scale) or illumination of a volume of fluid by a single frequency light such as Nd:YAG laser. Two consecutive images are taken at a known time interval and resulting images are compared using cross-correlation (two frames) or auto-correlation (single frame) algorithms. Micro PIV (μPIV) is a derivative of PIV technique adapted for micro flow visualization. First studies in the area of μPIV were conducted by Santiago et al. followed by Meinhart et al. (Figure 1) and Koutsiaris (Koutsiaris, Mathioulakis et al. 1999) and other researchers.

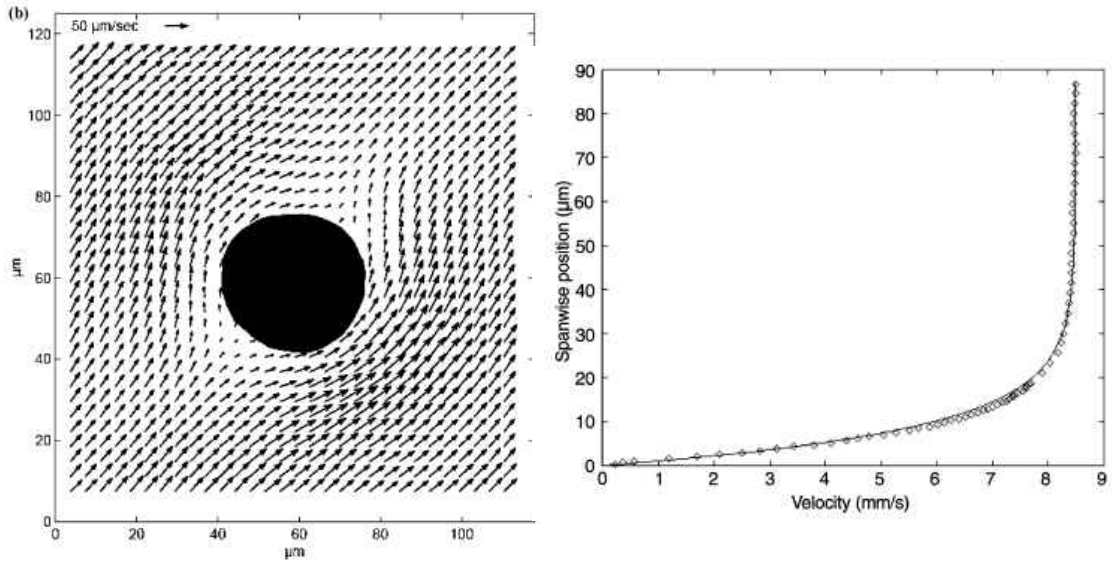

Figure 1 Pressure driven flow in a Hele-Shaw cell (Santiago et al.(Santiago, Wereley et al. 1998)); Right) μPIV flow visualization using ensemble-averaging measured in a nominally 300x300μm channel. The solid line is given by analytical solution (Meinhart, Wereley et al. 1999)

There are three key alterations from PIV to μPIV(Meinhart, Wereley et al. 1999):

First: since the flow passages are micron size; in this case, Brownanian motion can be a noise generating factor because the random motion of particles are in the order of the limited displacements of the particles due to the bulk motion of the fluid.

Second: dimension of flow passage are in micrometer range; hence the particles used for visualization are even smaller. Complications arise in imaging such particles that have diameters on the order of the illumination light wavelength (for example Nd:YAG laser produces 532 nm wavelength light).

Third: due to size limitations it is not possible to generate two-dimensional light sheets that only illuminate particles on a 2D plane inside the flow. Rather, a three dimensional volume is illuminated. In this case, particles above and below the focal plane get illuminated and eventually contribute to the noise. While out of focus particles are not in the same plane as the in-focus particles, yet they would contribute to the velocity

measurement algorithm. This issue is has been addressed in the present manuscript.The light coming from particles off the plane of focus forms a background noise (glow) which makes it difficult to distinguish between light coming from in-focus particles and that from the off-focus particles. Problems arising due to volume illumination issues in μPIV have been studied by (Meinhart, Wereley et al. 2000), (Olsen and Adrian 2000), (Ovryn 2000) and (Cummings 2000). Details of these studies are given in the dedicated chapter.

In the first chapter of this study, the effect of depth of focus and varying time intervals between images of a double-frame pair on the Ensemble cross-correlation μPIV scheme is found by using the backward facing step (sudden expansion) flow as the subject of flow imaging. Recirculation and vortex generation are distinct features of sudden expansion flows. Onset of recirculation and development of vortices has been studied using μPIV. Further more, this flow pattern has been used a subject to investigate technical parameters of the imaging system, namely the depth of focus and time intervals between pair images. As mentioned earlier, flow visualization is of key importance in studying flow behavior at reduced scales and investigation of issues related to μPIV - a major technique for flow imaging in micro flows - is useful and necessary.

Moving on to the applications of microfluidics, it is noted that in majority of cases especially in analytical lab on chips, mixing of two or more fluids is essential to achieving the application goals. Microfluidic devices are mainly designed for chemical and biological applications where rapid and efficient mixing is essential. Mixing is of considerable importance to realizing lab-on-a-chip (LOC) bio-analysis systems since a

majority of the applications often involve reactions that require quick and efficient mixing of reactants for initiation (Liu, Stremler et al. 2000). Nevertheless, mixing is greatly limited at the microscale where fluid flow is almost in all cases laminar. In laminar flows, layers of fluid co-flow and slide over their neighboring layers in a parallel manner without motion in the transverse direction. Considering the Highly laminar nature of flow and the fact that introduction of chaos and turbulence cannot be easily achieved or may not be practical under design constraints, it is expected that rapid mixing cannot be readily achieved in microfluidic devices. This limitation is the motivation for designing novel micromixing concepts.

Micromixer designs are categorized based on the source of energy used to perform mixing. Active mixers are stimulated by external sources of energy, while passive mixers achieve mixing based on geometrical design of the mixing channels (Nguyen and Wu 2005). In the former class, external sources such as acoustic (Liu, Yang et al. 2002), thermal (Tsai and Lin 2002), electrokinetic (Oddy, Santiago et al. 2001) and pressure disturbances (Deshmukh, Liepmann et al. 2001) cause stirring effects that enhance mixing of reagents (Figure 2). While active micromixers have better mixing performance compared to passive mixers, complications in integrating the external stimulus mechanisms and the required power sources into the microdevices make them expensive and incompatible to most applications; especially in cases where cheap disposable platforms are desired. Majority of passive mixers are designed based on various channel geometries in which external power sources are not required and the streaming flow itself creates mixing (Liu, Stremler et al. 2000; Lee, Kim et al. 2006). Due to fabrication and

cost issues, 2D (planar) passive micromixers are preferred over those with complex three dimensional structures (Jessica Melin 2004).

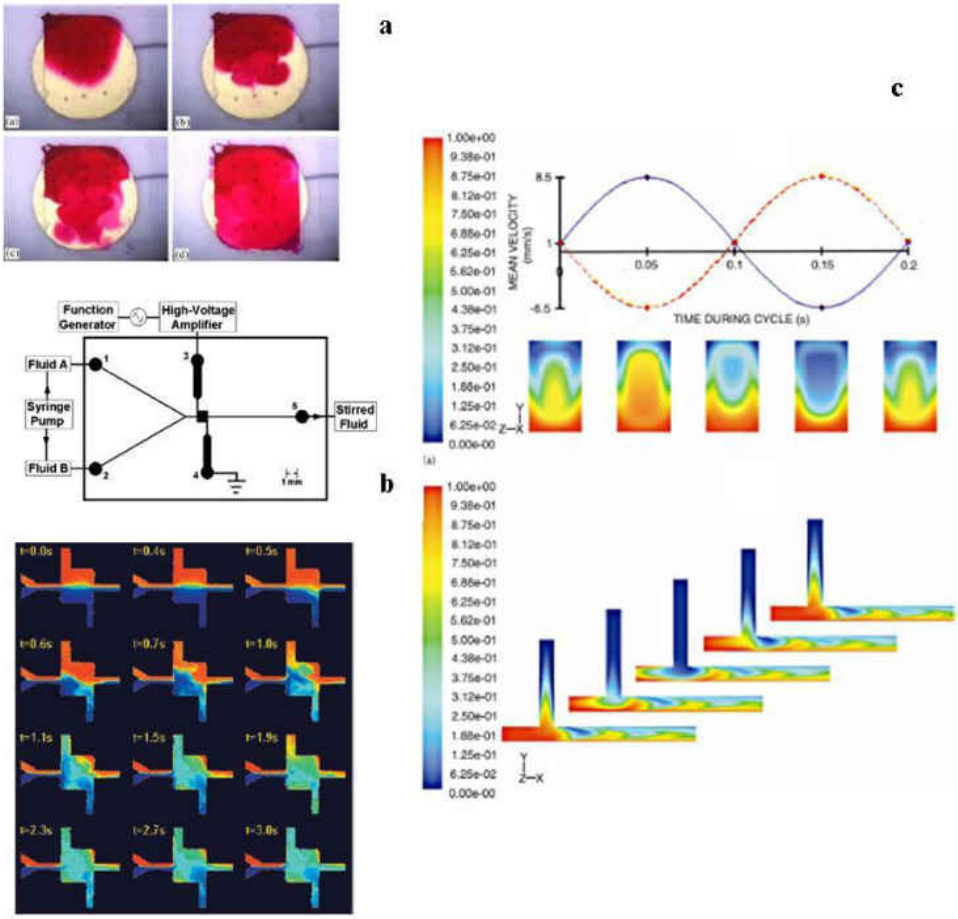

Figure 2 a) Acoustic mixing (Liu, Yang et al. 2002) b) Electrokinetic instability mixing (Oddy, Santiago et al. 2001) c) Mixing enhancement using time pulsing (Glasgow and Aubry 2003)

In the second chapter, micromixing has been studied theoretically and based on the findings an in plane passive micromixer has been designed, fabricated and tested for mixing performance. Numerical simulations were conducted to evaluate the mixing concept. Laminar velocity profile variation in the mixing channel is a key feature of the

mixer; μPIV studies developed in this study have been used to visualize the flow and verify the periodic variation of flow in the mixing device.

Fabrication of devices was done in the clean room facilities in-house. Details of fabrication, testing and image processing performed as part of the characterization are documented and given as appendices.

List of References

Basu, S., C. W. Wolgemuth, et al. (2004). "Measurement of Normal and Anomalous Diffusion of Dyes within Protein Structures Fabricated via Multiphoton Excited Cross-Linking." Biomacromolecules **5**(6): 2347-2357.

Brody, J. P., P. Yager, et al. (1996). "Biotechnology at low Reynolds numbers." Biophysical Journal **71**(6): 3430-3441.

Cummings, E. B. (2000). "An image processing and optimal nonlinear filtering technique for particle image velocimetry of microflows." Experiments in Fluids **29**(7): S042-S050.

Daniel, A. B. (2001). "Taylor dispersion of a solute in a microfluidic channel." Journal of Applied Physics **89**(8): 4667-4669.

Deshmukh, A., D. Liepmann, et al. (2001). Continuous micromixer with pulsatile micropumps. Solid-State Sensor and Actuator Workshop, Hilton Head Island.

Glasgow, I. and N. Aubry (2003). "Enhancement of microfluidic mixing using time pulsing." Lab Chip **3**: 114-120.

Huber, D. L., R. P. Manginell, et al. (2003). "Programmed Adsorption and Release of Proteins in a Microfluidic Device." Science **301**(5631): 352-354.

Jessica Melin, G. G., Niclas Roxhed, Wouter van der Wijngaart and Göran Stemme (2004). "A fast passive and planar liquid sample micromixer." Lab on a Chip.

Kandlikar, S. G. (2002). "Fundamental issues related to flow boiling in minichannels and microchannels." Experimental Thermal and Fluid Science **26**(2-4): 389-407.

Koutsiaris, A. G., D. S. Mathioulakis, et al. (1999). "Microscope PIV for velocity-field measurement of particle suspensions flowing inside glass capillaries." Measurement Science and Technology(11): 1037.

Lauga, E., M. P. Brenner, et al. (2007). Microfluidics: The no-slip boundary condition. Handbook of Experimental Fluid Dynamics (Chapter 19), Springer.

Lee, S. W., D. S. Kim, et al. (2006). "A split and recombination micromixer fabricated in a PDMS three-dimensional structure." Journal of Micromechanics and Microengineering **16**(5): 1067-1072.

Liu, R. H., M. A. Stremler, et al. (2000). "Passive Mixing in a Three-Dimensional Serpentine Microchannel." Journal of Microelectromechanical Systems **9**: 190-197.

Liu, R. H., J. Yang, et al. (2002). "Bubble-induced acoustic micromixing." Lab on a Chip **2**: 151-157.

Lockerby, D. A., J. M. Reese, et al. (2004). "Velocity boundary condition at solid walls in rarefied gas calculations." Physical Review E **70**(1): 017303.

Meinhart, C. D., S. T. Wereley, et al. (2000). "Volume illumination for two-dimensional particle image velocimetry." Measurement Science and Technology(6): 809.

Meinhart, C. D., S. T. Wereley, et al. (1999). "PIV measurements of a microchannel flow." Experiments in Fluids **27**(5): 414-419.

Moseler, M. and U. Landman (2000). "Formation, Stability, and Breakup of Nanojets." Science **289**(5482): 1165-1169.

Nguyen, N.-T. and Z. Wu (2005). "Micromixers-a review." Journal of Micromechanics and Micorengineering **15**: R1.

Oddy, M. H., J. G. Santiago, et al. (2001). "Electrokinetic Instability Micromixing." Analytical Chemistry **73**(24): 5822-5832.

Olsen, M. G. and R. J. Adrian (2000). "Out-of-focus effects on particle image visibility and correlation in microscopic particle image velocimetry." Experiments in Fluids **29**(7): S166-S174.

Ovryn, B. (2000). "Three-dimensional forward scattering particle image velocimetry applied to a microscopic field-of-view." Experiments in Fluids **29**(7): S175-S184.

Santiago, J. G., S. T. Wereley, et al. (1998). "A particle image velocimetry system for microfluidics." Experiments in Fluids **25**(4): 316-319.

Sinton, D. (2004). "Microscale flow visualization." Microfluidics and Nanofluidics **1**(1): 2-21.

Stone, H. A., A. D. Stroock, et al. (2004). "ENGINEERING FLOWS IN SMALL DEVICES: Microfluidics Toward a Lab-on-a-Chip." Annual Review of Fluid Mechanics **36**(1): 381-411.

Thorsen, T., R. W. Roberts, et al. (2001). "Dynamic Pattern Formation in a Vesicle-Generating Microfluidic Device." Physical Review Letters **86**(18): 4163.

Tieu, A. K., M. R. Mackenzie, et al. (1995). "Measurements in microscopic flow with a solid-state LDA." Experiments in Fluids **19**(4): 293-294.

Tsai, J.-H. and L. Lin (2002). "A thermal-bubble-actuated micronozzle-diffuser pump." Journal of Microelectromechanical Systems **11**(6): 665-671.

Yi-Kuen, L., J. Deval, et al. (2001). Chaotic mixing in electrokinetically and pressure driven micro flows. Micro Electro Mechanical Systems, 2001. MEMS 2001. The 14th IEEE International Conference on.

CHAPTER ONE: SUDDEN EXPANSION STEP FLOW IN A MICROCHANNEL

Introduction

Particle Image Velocimetry (PIV) can be used to obtain high-resolution 2-D velocity fields (Meinhart, Wereley et al. 1998). In conventional PIV, the flow is seeded with tracer particles that scatter light due to having a refractive index different from that of the fluid or because of fluorescence properties. Laser light is usually used as a source of illumination. By means of the special configuration of optics, the flow is illuminated in a 2D light sheet at the desired location of the flow. The tracer particles, which reasonably follow the fluid flow, are photographed at consecutive instances with a known time interval. Each pair of the double-frame image is subdivided into smaller regions called the interrogation spots. The displacement of the particles within the interrogation spot is derived based on statistical methods with high accuracy (0.1 pixels) which results in visualization of the velocity field in the illuminated 2D plane with knowledge of the time interval (Nguyen and Wereley 2002).

Micro particle image velocimetry (μPIV) is a useful tool in studying fluid mechanics at the reduced scale (micrometer range) also known as microfluidics. In conventional PIV, with the proper selection of optics, it is possible to illuminate particles in the flow on a desired 2D plane. The thickness of the illumination light sheet is much smaller than the characteristic dimensions of the flow; for example the width/height of a duct. Therefore, the flow can be analyzed layer by layer. In μPIV however, all the particles in the flow field are illuminated due to limited optical access; the intensity of light picked up by the tracer particles varies depending on how far away they are from the plane of focus. Epi-fluorescence technique is implemented in μPIV, since the limited optical access does not

allow illumination and collection of the excitation and re-emission light from two separate paths. Fluorescent dyes offer the possibility of using only one optical pathway. Excitation light from an Nd:Yag laser with a fixed wavelength is guided to the desired location of the flow; fluorescent dyes absorb this light moving into an excitation mode; at releasing the absorbed energy, they re-emit light at a higher wavelength, since part of the original energy gets dissipated as heat. The re-emission light can be filtered out using a dichroic mirror that is transparent to the wavelength used for excitation but reflective to the re-emission wavelength. The re-emission light is guided to the CCD camera where the images are recorded in pairs and eventually transmitted to a computer for further processing (Figure 3).

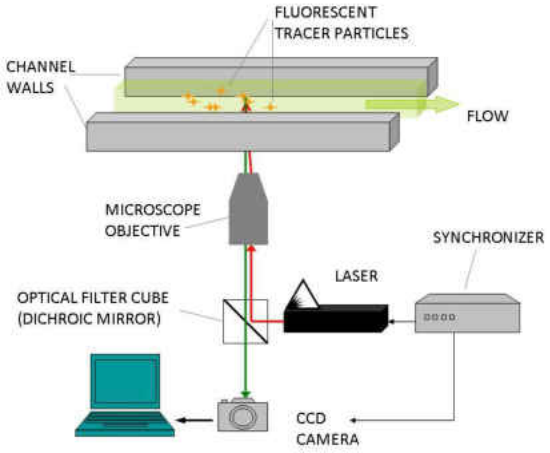

Figure 3 Micro particle image velocimetry setup

The fact that all particles in the field of view are illuminated and contribute to the final image can be a major problem. The light from particles off the plane of focus forms a background noise (glow) which makes it difficult to distinguish between light coming from in-focus particles and that from the off-focus particles. Micro particle image

velocimetry technique is different from the conventional PIV in three ways; 1) tracer particles are in the size range of the wavelength of the illumination light, which can make the visualization of microflows challenging; 2) Brownian random motion of tracing particles can be a significant source of error in low rates of flow 3) illumination of the flow is not in a 2D plane but is rather an illumination volume; hence, out of focus emissions from particles below and above the depth of focus increase the noise to signal ratio. Santiago et al. first used PIV for microfluidic flows by using the concept of epi-fluorescence (Santiago, Wereley et al. 1998). Due to the extremely small dimensions and complexities of flow measurement in small scales (micro and nano meter scales), not many successful experimental studies have been conducted that give details of the flow such as the velocity and pressure fields and their derivatives. However, Devasenathipathy, Santiago et al. 2002, Santiago and Meinhart Santiago, Wereley et al. 1998 have characterized such flow patterns in the micron scale devices.

In the present work, fluorescent dyed polystyrene tracer particles with an average diameter of 1.1 μm were used. The absorption wavelength peak is 540nm and re-emission is at a longer wavelength of 560nm for these particles. The emission light level is affected by the fluorophore concentration, particle size, illumination wavelength, pulse energy, pulse duration and the optical filters. The illumination source used here is a Q-switch Nd-Yag laser that generates 532nm wavelength light. With the epi-fluorescent technique the illumination and re-emission light to and from the measurement location, have identical pathways except after the epi-fluorescence filter cube. The filter cube containing a dichroic mirror and barrier filter is used to direct the illumination light and the re-emission light to and from the fluorescent particles so that the fluorescent re-emission

gets filtered out and guided to the CCD camera which records the images and transmits them to a computer for processing. Increasing the fluorescent particle concentration will increase the concentration of particles in the image, but since a volume of fluid is illuminated rather than a 2D sheet, light picked up from out of focus particles may increase the background noise level. The laser light pulse duration is fixed to a value between 3 to 10 nano-seconds. Increasing laser pulse energy also increases the emission level but only to a certain threshold level after which no additional emission will be added. The double frame image pairs are further processed with cross correlating algorithms and the velocity vector field is derived. Ensemble correlation processing is used which is appropriate for visualization of steady flow patterns. Double-frame image pairs obtained in μPIV are processed by cross-correlation schemes which are often written in the form of a computer code in order to resolve the velocity field from the motion of the vase number of illuminated particles. The purpose of this study is to evaluate the sensitivity of the Ensemble Cross-correlation algorithm to the optical focus depth and variation of time intervals between image pairs. This scheme is mostly used for processing steady flows. The correlation function at a certain interrogation spot is generally represented by the following set of equations (Gad-el-Hak 2005):

$$\Phi_k(m,n) = \sum_{j-1}^{q} \sum_{i-1}^{p} f_k(i,j).g_k(i+m, j+n) \quad \mathbf{1}$$

Where f and g are the gray value of the gray value distribution from the first and second exposure for the k^{th} recording PIV recording pair for an interrogation spot of size (p x q) pixels. The highest peak of this function occurs at the particle image displacement in the interrogation spot. If the flow has a steady characteristic, then the main peak of $\Phi_k(m,n)$ always occurs at the same position for PIV recording pairs recorded at different times,

whereas all other sub-peaks occur with random intensities and positions in different recording double frame pairs. If a large number of pairs is taken together (ensemble) and averaged, then the main peak will remain at the same location and the random peaks (noise) will average out to zero. The average (ensemble) correlation is given as

$$\Phi_{ens}(m,n) = {}^{1}\!/_{N}\sum_{k-1}^{N}\Phi_{k}(m,n)$$

Once the displacement is found in an interrogation spot, given the time interval[2] the velocity vectors can be plotted. Fifty pair images were required on average to yield quality vector fields. The time interval between frames of a pair depends on the magnitude of the velocity of the tracer particles. It is noted that if the velocities in the photographed area vary significantly compared to each other, then different time intervals should be used to capture various ranges of velocity magnitudes; for example, small time intervals are required to track fast moving tracer particles and larger time intervals to capture the slow moving tracers.

Problem Statement

In conventional PIV, with the proper selection of optics, it is possible to illuminate particles in the flow on a desired 2D plane. The thickness of the illumination light sheet is much smaller than the characteristic dimensions of the flow; for example the width/height of a duct. Therefore the flow can be analyzed layer by layer. In μPIV however, all the particles in the flow field are illuminated due to limited optical access; the intensity of light picked up by the tracer particles varies depending on how far away they are from the plane of focus. Epi-fluorescence technique is implemented in μPIV, since the limited optical access does not allow illumination and collection of the excitation and re-emission light from two separate paths. Fluorescent dyes offer the possibility of using only one

optical pathway. Excitation light from an Nd:Yag laser with a fixed wavelength is guided to the desired location of the flow; fluorescent dyes absorb this light moving into an excitation mode; at releasing the absorbed energy, they re-emit light at a higher wavelength, since part of the original energy gets dissipated as heat. The re-emission light can be filtered out using a dichroic mirror that is transparent to the wavelength used for excitation but reflective to the re-emission wavelength. The light from particles off the plane of focus forms a background noise (glow) which makes it difficult to distinguish between light coming from in-focus particles and that from the off-focus particles. Olsen and Adrian (Olsen and Adrian 2000; Olsen and Adrian 2000) introduced the concept of particle visibility for μPIV measurements while addressing this issue. Particles were considered to be visible if only their peak intensity in the recorded images rose significantly above the background glow. Particle visibility was found to be weakly dependent on magnification, and most readily increased by decreasing the *f* number of the optical system; depth-of-field increases with increasing the f-number. This means that images taken with a low f-number will tend to have limited number of particles in focus, with the rest being out of focus; hence eliminating the contribution of non-visible (out of focus particles) to the image. If the optical parameters are kept constant, then particle visibility can be increased by either decreasing the depth of the microfluidic device or using a lower particle concentration. However, using lower particle concentration will have the effect of reducing the number of particles within each interrogation volume resulting in noisier velocity estimates. In addition, reduced concentration of fluorescent dye can possibly necessitate using larger interrogation spots resulting in lower spatial resolution. Meinhart et al. (Carl, Steve et al. 2000; Meinhart, Wereley et al. 2000)

maintained high spatial resolution at low particle concentration by taking many realizations and then averaging the calculated spatial correlations for each interrogation region to yield a high-vector-density velocity field. This technique is limited to steady flows or periodic flows with phase locking. It is important to note that usually the measured velocity is found to be a *weighted average over the depth* of the fluidic device. By using appropriate weighting functions, velocity variation from top to bottom of the interrogation volume can be accounted for. The weighting function can be used to put a bound on the interrogation volume (depth of correlation) by defining a distance from the object plane beyond which particles no longer contribute to the correlation function significantly. As a solution for the background noise reduction, Bourdon et al. (Bourdon, Olsen et al. 2004) proposed an image filtering method, termed power-filtering for controlling the depth of correlation, independent of the image acquisition system, particle size, and flow characteristics. By choosing appropriate power values, it is possible to increase or decrease the depth of correlation by a factor two.

In this study, the effect of depth of focus and varying time intervals between images of a double-frame pair on the Ensemble cross correlation scheme is found. Backward facing step in a rectangular cross section microchannel having a hydraulic diameter of 133 microns, by means of the particle image velocimetry technique and implementing the Ensemble method.

Recirculation and flow separation is the main feature of flow at sudden expansion geometries in internal macroscopic flows. This unique flow pattern offers an opportunity to investigate the characteristics of the above mentioned scheme in resolving velocity profiles in microchannels. Sudden expansion (backward facing step) flows are among

commonly encountered basic flow patterns that have been addressed widely by researchers by means of theoretical, numerical and experimental methods in laminar and turbulent flow regimes in the macro-scale. Flow created at backward facing steps is of importance because it gives insight to many internal flow patterns generated at geometries containing sudden expansions in the path of flow; phenomena such as flow separation and recirculation and their effects on heat and mass transfer can be analyzed with reference to this flow pattern. Armaly et al. (Armaly, Durst et al. 1983) used Laser-Doppler anemometry to make comprehensive measurements on air flows over a backward facing step in a test channel over a 70-8000 range of Reynold's number covering laminar, transitional, and turbulent flows. Many numerical works have also been reported on this subject. Biswas et al. (Biswas, Breuer et al. 2004) studied the backward facing step flow for expansion ratios of 1.95, 2 and 3 and provided information on characteristic flow patterns for Re of 10^{-4} to 800.

Here, the effect of variation of the depth-of-focus applied by adjusting the microscope focus and the time intervals between PIV image-pairs is found on the flow visualization using μPIV. Results at transition to recirculation flow for backward facing step for a 1:5 expansion is also provided.

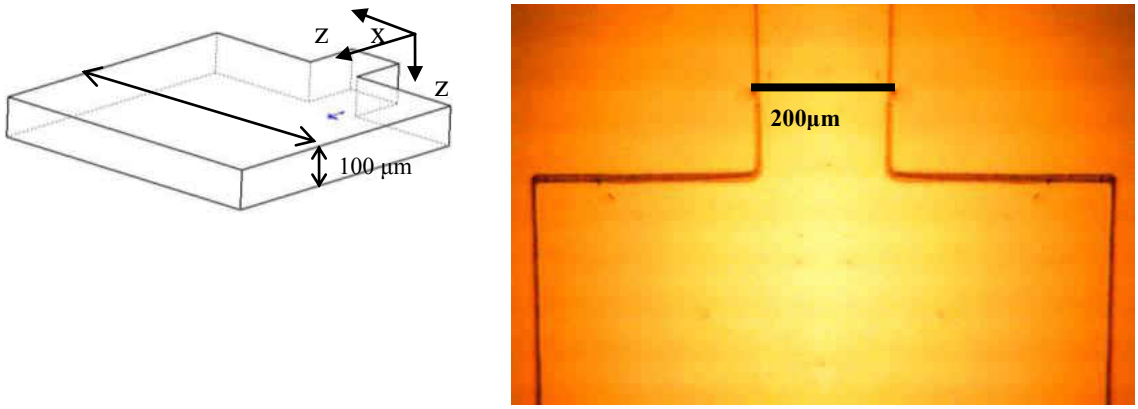

Figure 4 Schematic of a sudden expansion feature in a microchannel (left), top view of an actual fabricated channel (right)

Experimental Setup

The microfluidic device used for this study is fabricated using the well established SU-8 photolithography and Polydimethylsiloxane (PDMS) replication techniques (Jo, Van Lerberghe et al. 2000). The device pattern is transferred via photolithography from a mask onto the silicon wafer which has been spin-coated with SU-8 photoresist. The developed SU-8 on the wafer is used as a mold; PDMS with a curing agent is poured on the mold and allowed to cure overnight at room temperature. The PDMS layer with cast features is then bonded to another flat piece of PDMS or glass slide by plasma surface treatment. The device consists of a straight channel with a rectangular cross section that suddenly expands to a larger width (1:5 ratio). Recirculation flow occurs as the flow suddenly expands. The width to height ratio is 10:1 (x: flow direction, z: depth) downstream the expansion (Figure 4). Since the bottom and top walls influence the flow due to the no slip boundary condition, then choosing the appropriate depth of focus would be a determining factor on the flow profile; this gives significance to the depth-of-focus. For example, closer to the walls, the vortex would have smaller radius with lower velocity magnitudes compared to the center portion that is less influenced by the walls.

The μPIV (TSI Inc. MN) apparatus consisted of the following major components; Nd:Yag laser source that generates green light at a wavelength of 532nm. Nikon (TE2000-S) inverted microscope is used for magnifying the flow field which is compatible with the epi-fluorescent technique (Figure 5).

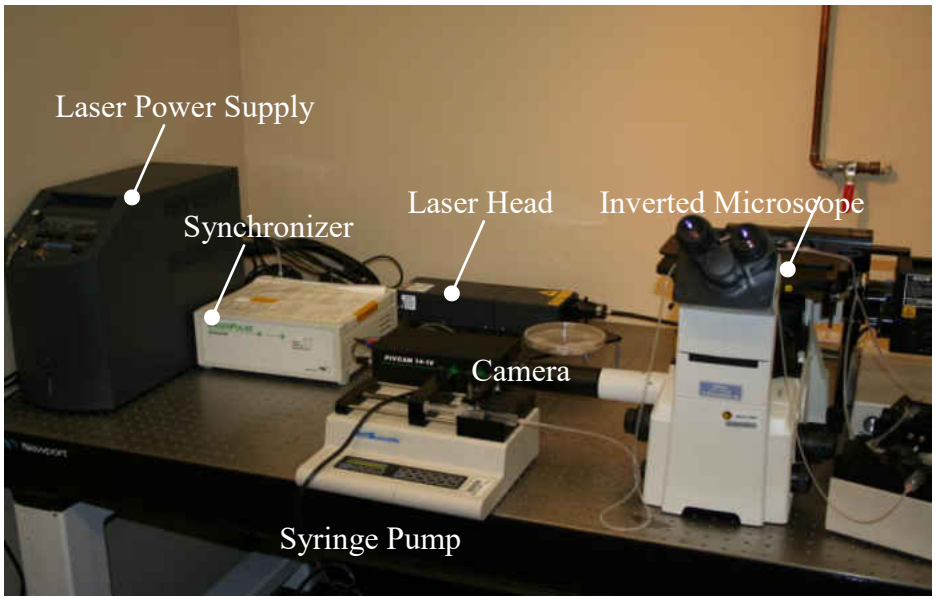

Figure 5 TSI microPIV equipment

A 10x magnifying objective lens was used. A barrier filter cube was used to filter out the re-emission light from the excitation light. Polystyrene fluorescent dye was used in this study as the tracer particle with the following properties: 1μm average diameter, 540nm excitation /560nm re-emission wavelength, 10^{10}beads/mL (FluroSpheres, Invitrogen CA). A CCD camera was used to capture PIV images, capable of acquiring image-pairs at maximum 15 double-image frames per second, with time intervals between two images of a frame as low as 1μs. The timings of the laser firing and image capture are controlled by a synchronizer unit. Ensemble cross correlation scheme together with background conditioning was used for deriving the flow field from the captured images. An average

of N=50 double-frame image pairs were processed for each case of variable time interval, depth of focus or change in flow rate. Flow through the microchannels is maintained and controlled by a precision syringe pump (KD Scientific, MA). Flow rate is varied such that the onset and development of recirculation is observed at the backstep feature. The effect of each variable is systematically investigated by maintaining all other variables and parameters constant.

Results

A typical characteristic of sudden expansion flows is the vortices and recirculation flow generated downstream the expansion feature. In microfluidic devices however, the circulation zone is absent in the typical range of micro-flows ($Re=\rho UD_H/\mu= 0.01\text{-}10$).$\rho$ and μ are density and viscosity of the fluid where U and D_H are average flow velocity and hydraulic diameter, respectively., laminar flow without any disturbances (Re=28) and a fully developed recirculation (Re=280) are shown in (Figure 6, Figure 7), respectively. All experiments were carried out using identical tracer particle concentrations. Each variable was varied holding the others constant. The hydraulic diameter is calculated for the rectangular cross section at the entrance channel, upstream of the expansion feature.

$$D_H = 4A/P \qquad (3)$$

Where A and P are the area and perimeter of the cross section, respectively. Note that for visualizing of each portion of the flow, depending on the magnitude of velocity, appropriate time intervals should be used. For example, in figure 6, the fast moving core is recorded using 75μs time interval, whereas for the slow moving flow at the corners away from the center, time intervals of 200 and 600 micro seconds, were used in section B and C respectively.

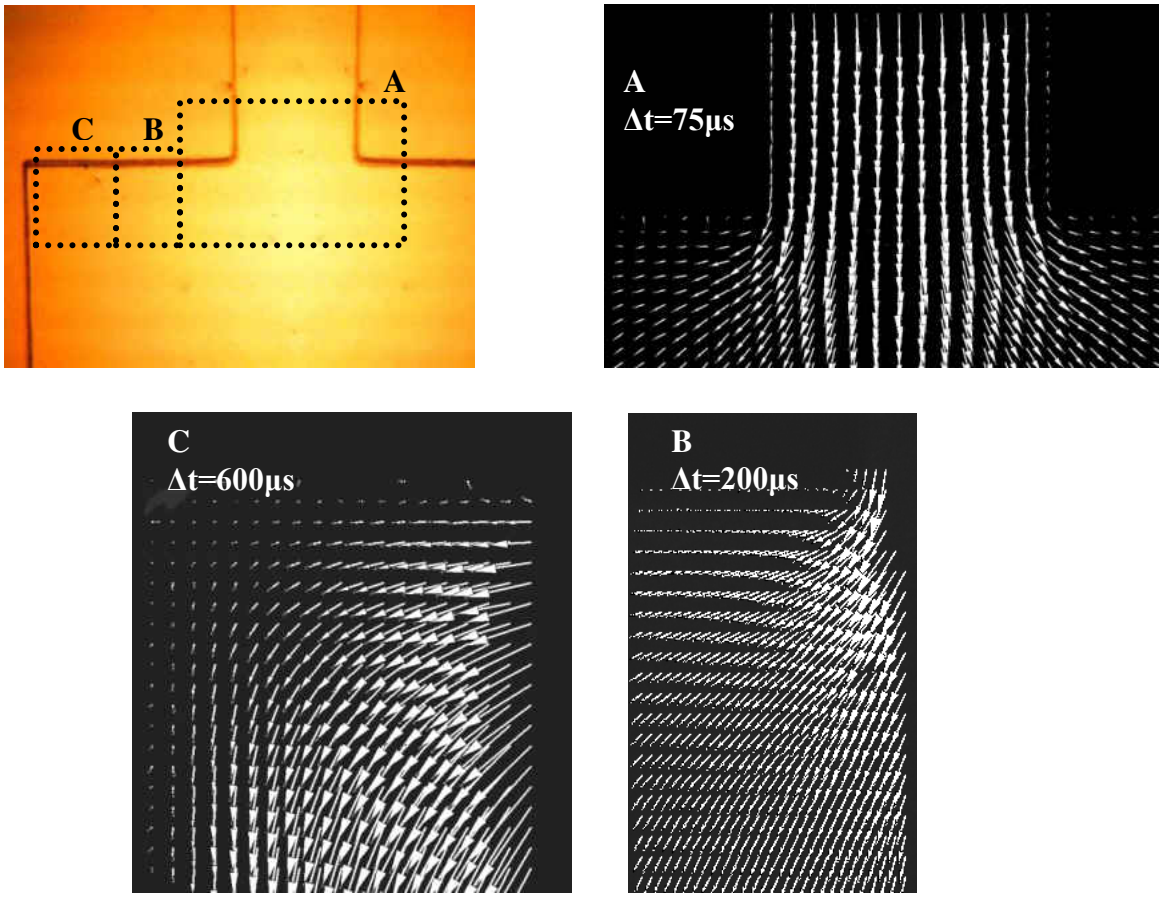

Figure 6 Laminar flow at a sudden expansion (1:5) feature; due to significant difference in the velocity magnitude, sections A, B and C were recorded using appropriate time interval (Δt) values (Re=28)

The first signs of recirculation appear at a flow rate of 950μL.min^{-1}. Using physical properties of water and the hydraulic diameter as the characteristic length, the corresponding Reynolds number, Re=95 at the onset of recirculation at the given plane of flow. It should be noted that the critical Re can vary from one plane to another with a different depth (z) since the flow has 3D structure. This range of Re numbers is fairly large, compared to typical microfluidic flows.

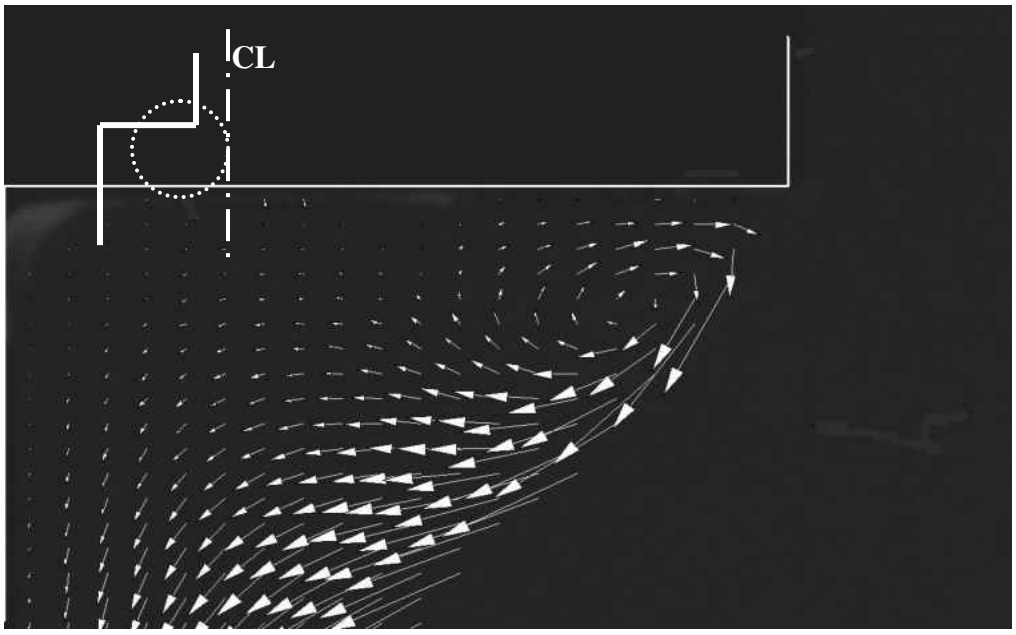

Figure 7 Recirculation zone developing at the backstep wall (Re=280)

Onset of Recirculation

Holding the depth of focus, time interval and other parameters constant, the flow rate was increased in increments of 100μL.min^{-1}. In (Figure 8), the evolution of the recirculation is shown as the flow rate is increased. Around Re=95 – 105 first signs of recirculation were observed at the backstep wall for the mid-plane. It should be noted that expansion ratio of 1:5 is a potentially-favorable geometrical factor for recirculation to occur; however, a fairly large flow rate is required to cause disruption of the orderly laminar flow. This reconfirms the highly viscous-dominated nature of flow in microfluidic devices. The recirculation first begins at the backstep wall where it further develops and gets bigger, influencing a larger radius of the flow. The streamlines show that as the flow rate is increased, a bigger portion of the flow is affected by the enlarging recirculation zone. The streamline that divides the circulating and non-circulating portions of the flow, initially

terminates on the backstep wall; this streamline migrates towards the sidewalls and moves downstream of the channel as the flowrate is further increased.

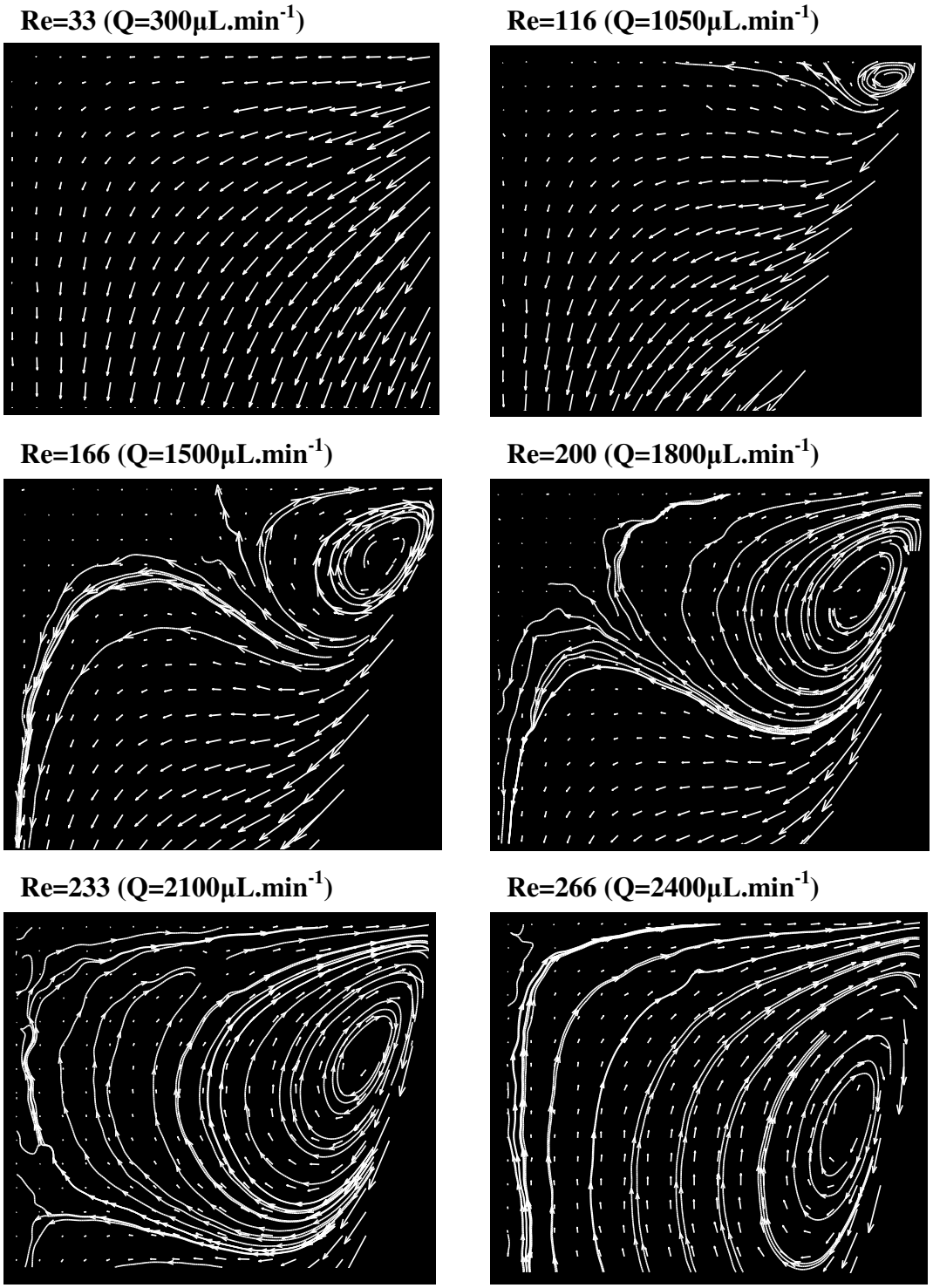

Figure 8 Initiation and development of a recirculation zone

The location where this dividing streamline meets the wall is called the reattachment zone. Figure 9 shows migration of the reattachment point from the backstep wall onto the sidewalls and further downstream as the flowrate is increased. This observation leads to the conclusion that the flow separation from the wall is absent in majority of microfluidic devices because such high flow rates corresponding to critical Re numbers rarely occur. This is in contrast to flows at sudden expansions in conventional dimensions with similar geometrical ratios.

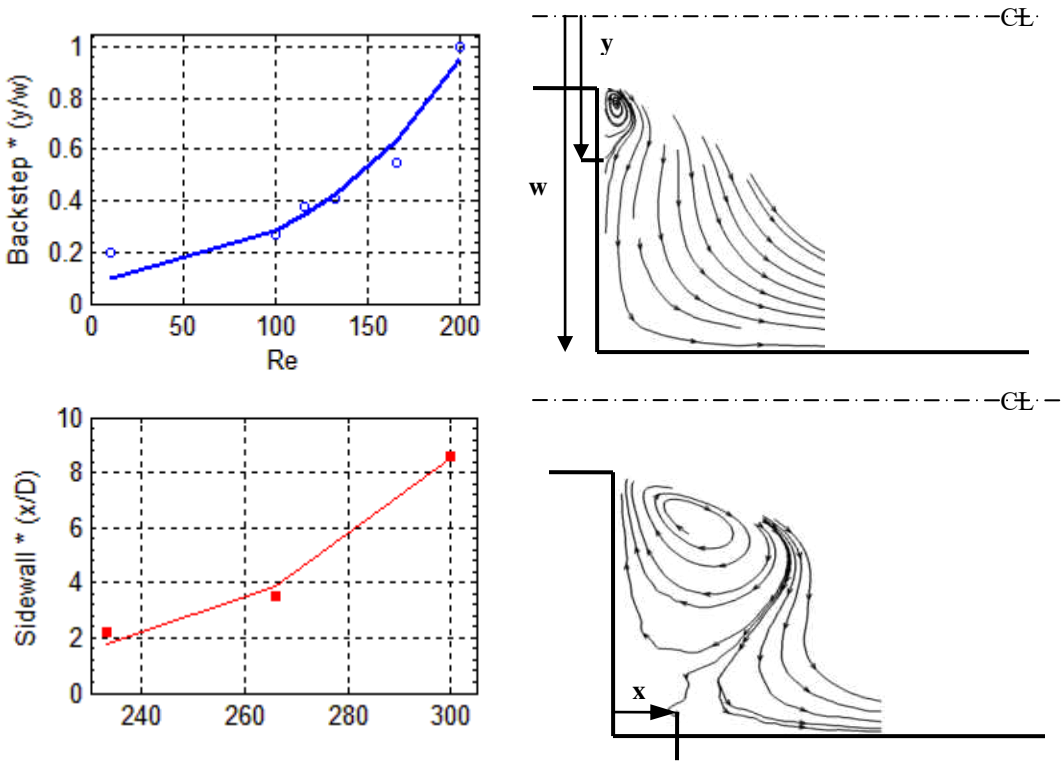

Figure 9 Evolution of the recirculation zone; the dividing streamline migrates from the backstep wall onto the sidewall of the channel and further downstream as flow rate increases

Effect of Depth of Focus

The microscope settings were adjusted to traverse the depth of the microchannel from top to bottom. The spin-coating speed of SU8 on the silicon wafer determines the thickness of the film. As mentioned earlier the patterns transferred to the SU8 film via photolithography, serves as the mold which is eventually used to cast the patterns onto

the PDMS resin to form the microchannels. The device height in this study was in the range of 100 to 120 μm; height variation is due to variations in the fabrication process such as spin coating. The tracer particles used for μPIV were dispersed homogenously in water and fed into the devices using an infusion pump. The same mixture with identical tracer particle concentration was used for all the test cases. The size of the tracer particles (1μm on average) is much smaller than typical dimensions of the flow such as the width and height of the device which ensures that the particles would follow the flow reasonably well. The border of the channels, as observed through the microscope, consists of a line with two edges; each representing the intersection of the sidewall with the top and the bottom wall. By adjusting the objective lens to be focused on the upper or lower bounds of the channel, one of those two lines would appear sharp and the other blurry (sidewall is not perfectly vertical). In this way, it is possible to pinpoint the upper and lower walls and calibrate the markings on the microscope focusing knobs with the actual microchannel depth. In (Figure 10), a series of PIV realizations are shown which correspond to various depths from the top to bottom of the microchannel. It is observed that given a preset time-interval (Δt=100μs) and flow rate, the resulting images from the correlation algorithm show almost the same flow pattern. This is an important finding since we explained earlier that with regards to the dimensions of the device, the top and bottom walls would certainly affect the flow field and that the flow is a function of the depth coordinate (3D flow).

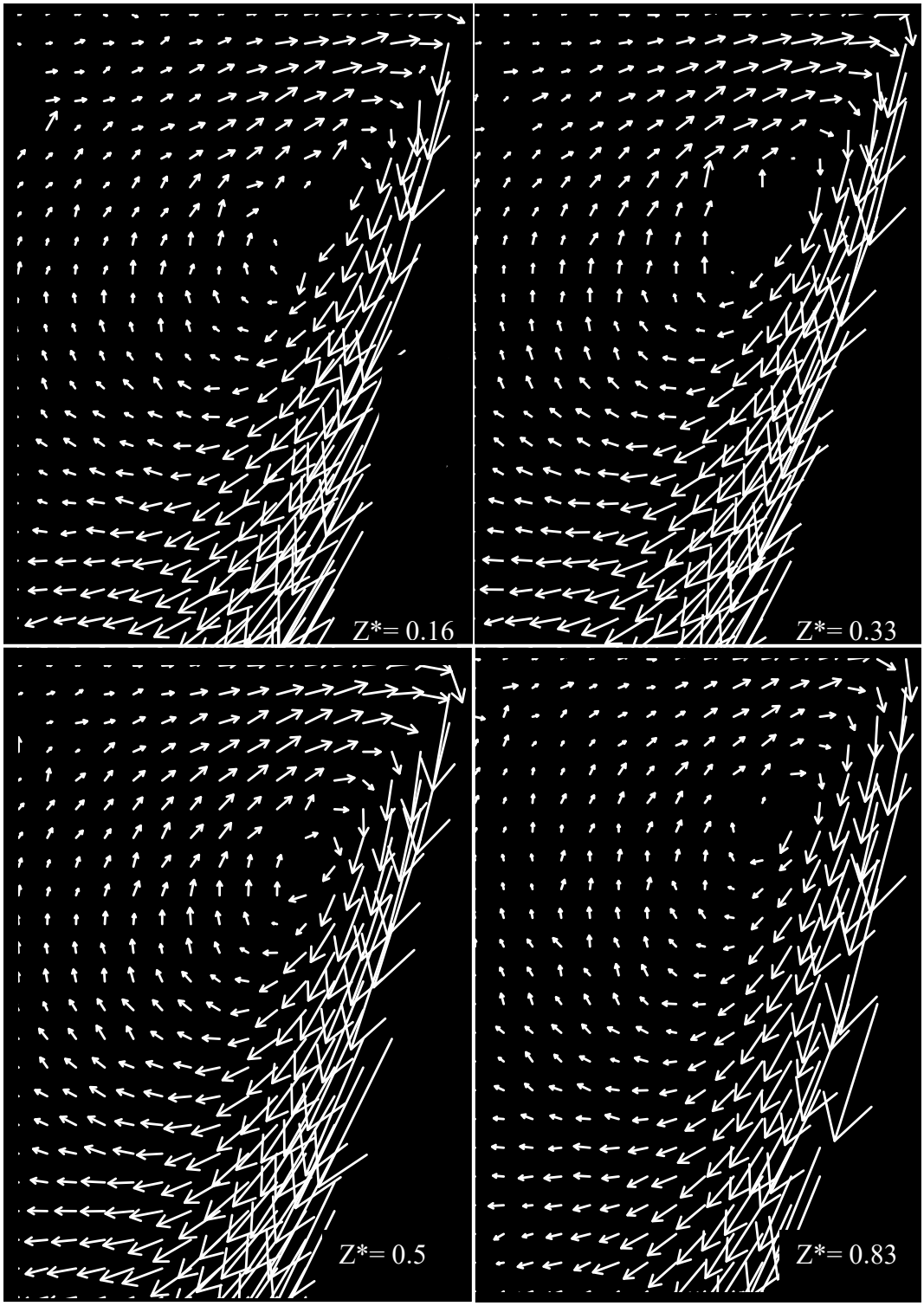

Figure 10 µPIV realizations of a recirculation flow at various depths of focus from top to bottom of the device; (Z*=z/H, D100µsec, Re=222); variation of depth of focus has insignificant effect on the output flow profile.

It was observed that except for a slight change in the resolution and overall quality of the images, the recorded flow fields are identical at various depth-of-focus values. This leads to the conclusion that the "ensemble cross correlation algorithm" is less sensitive to the depth of focus. if not so, then the flow patterns resulting from using different values of depth-of-focus should have been different.

Effect of Time Interval between PIV Image-Pairs

In order to investigate the effect of time intervals (Δt) between PIV recordings of image-pairs, the depth of focus, flow rate and other parameters were set as constants and various time intervals were chosen. The μPIV results for a given flow rate and depth are expected to have a steady flow pattern regardless of imaging time interval at least qualitatively. From (Figure 11), it can be concluded that the cross correlation algorithm is highly sensitive to the time interval used for PIV recording of image-pairs. It was observed that depending on the value chosen for the time interval, the algorithm gets locked into a plane of flow that can be resolved within the range of parameters chosen, and which results in the most frequently occurring displacement peaks over the averaged image-pairs, regardless of the depth of focus. Note that the flow rate and depth of focus are held constant and at least qualitatively similar flow patterns should have been observed using a constant flow rate and depth-of-focus. However, the flow fields resulting from the three cases are significantly different in terms of qualitative flow patterns as well as quantitative values of the velocity magnitudes. Layers of fluid moving closer to the top and bottom walls have lower velocity magnitudes compared to those close to the center of the channel due to the no slip condition; larger time intervals are required to resolve

slow moving layers while for the faster moving layers at the core of the flow, shorter time intervals should be used.

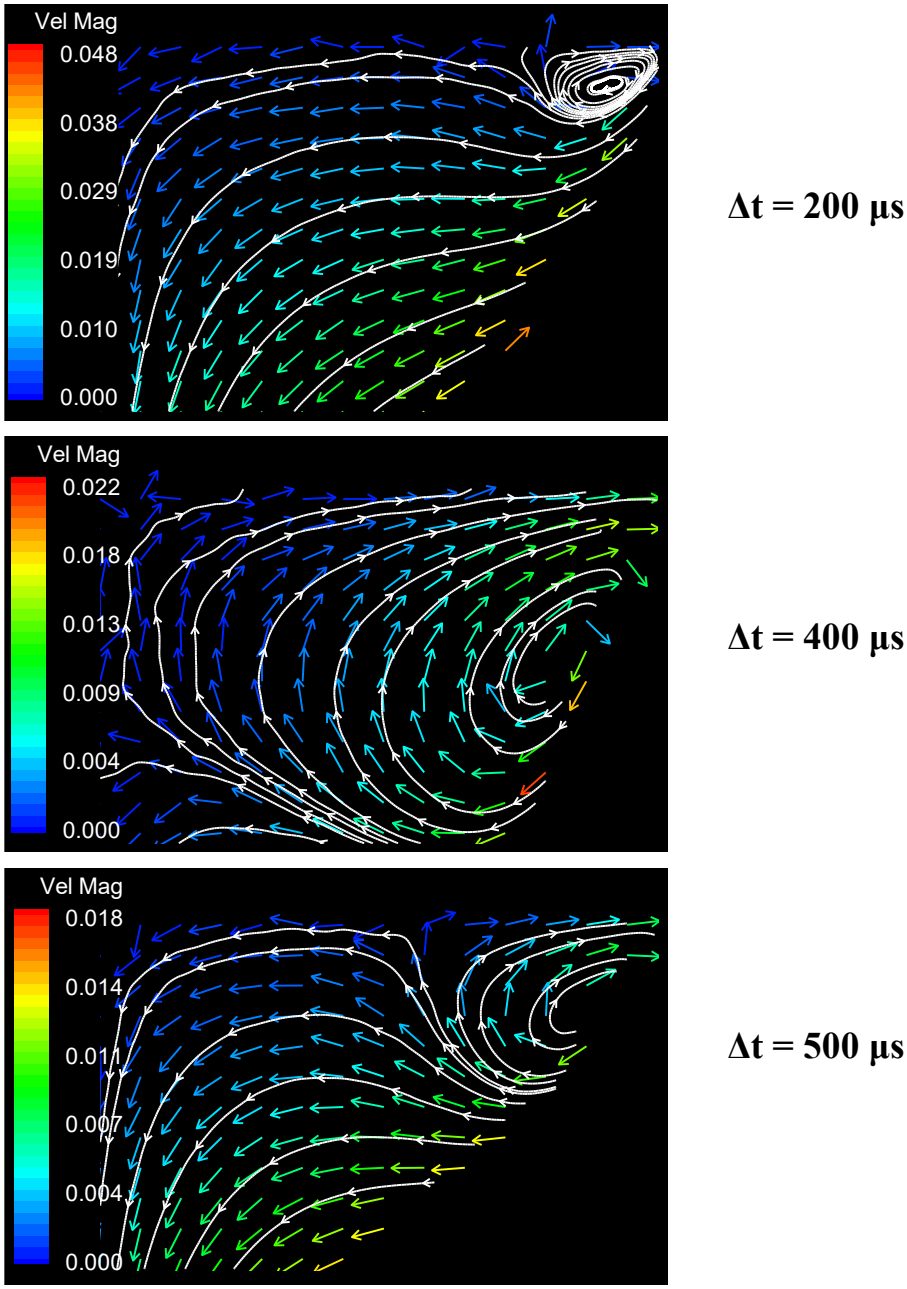

Figure 11 µPIV realizations using different values of time interval (Dt) between recordings of the PIV image pairs; depth of focus (Z*=0.5) and flow rate (Re=222) were held constant. Resulting flow patterns differ qualitatively and quantitatively.

In this sense, there can be an indirect correlation between the depth at which the flow field is computed and the time interval used to record that flow field.

Conclusion

Backward facing step flow was visualized in a 1:5 expansion ratio in a microchannel using the μPIV technique. The device was fabricated using the well established SU8 lithography and PDMS soft lithography fabrication process. Three variables were investigated while making flow visualizations. First, the flow rate was increased in increments to find out the onset of vortex generation and emergence of flow recirculation zones. The behavior of the vortex in a given plane of flow was investigated and migration of the dividing streamline was observed; the dividing streamline initially resides on the backstep wall and gradually shifts on to the sidewall and moves downstream as the flow rate is further increased. It was concluded that the flow hardly gets separated from the wall in normal flow rates used in microfluidic devices even with geometrically favorable features for recirculation and separation to occur. The onset of recirculation was observed at relatively large flow rates. This reconfirms that the fluid flows are highly ordered and laminar at reduced scales and cannot be disrupted easily. Second, the effect of depth of focus was studied on the μPIV visualizations. It was observed that the cross-correlation algorithm used in this study (ensemble cross correlation) was not sensitive to the exact focusing of the optics on a given plane of flow as long as long as the focus remained within the upper and lower bounds of the microchannel. Finally, it was observed that the algorithm is highly affected by the value of time intervals used for recording PIV double image-pairs. In other words, with a given time interval, only that portion of the flow which yields the most repeated displacement peaks in the interrogation spots is resolved

as the final output. By considering a set of μPIV realizations using incremental time intervals and combining them together, an indirect method for resolving the depth coordinate of the flow (often a challenging subject) in μPIV realization using ensemble cross correlation schemes.

List of References

Armaly, B. F., F. Durst, et al. (1983). "Experimental and theoretical investigation of backward-facing step flow." Journal of Fluid Mechanics **127**: 473-496.

Biswas, G., M. Breuer, et al. (2004). "Backward-Facing Step Flows for Various Expansion Ratios at Low and Moderate Reynolds Numbers." Journal of Fluids Engineering **126**(3): 362-374.

Bourdon, C. J., M. G. Olsen, et al. (2004). "Power-filter technique for modifying depth of correlation in microPIV experiments." Experiments in Fluids **37**(2): 263-271.

Carl, D. M., T. W. Steve, et al. (2000). "A PIV Algorithm for Estimating Time-Averaged Velocity Fields." Journal of Fluids Engineering **122**(2): 285-289.

Devasenathipathy, S., J. G. Santiago, et al. (2002). "Particle Tracking Techniques for Electrokinetic Microchannel Flows." Anal. Chem. **74**(15): 3704-3713.

Gad-el-Hak, M. (2005). The MEMS Handbook, CRC Press.

Jo, B.-H., L. M. Van Lerberghe, et al. (2000). "Three-dimensional micro-channel fabrication in polydimethylsiloxane(PDMS) elastomer." Journal of Microelectromechanical Systems **9**(1): 76-81.

Meinhart, C. D., S. T. Wereley, et al. (2000). "Volume illumination for two-dimensional particle image velocimetry." Measurement Science and Technology(6): 809.

Meinhart, C. D., S. T. Wereley, et al. (1998). Micron-resolution velocimetry techniques. Developments in laser techniques and applications to fluid mechanics. R. J. A. e. al. Berlin, Springer Verlag.

Nguyen, N.-T. and S. T. Wereley (2002). Fundamentals and applications of microfluidics, Artech House.

Olsen, M. G. and R. J. Adrian (2000). "Brownian motion and correlation in particle image velocimetry." Optics & Laser Technology **32**(7-8): 621-627.

Olsen, M. G. and R. J. Adrian (2000). "Out-of-focus effects on particle image visibility and correlation in microscopic particle image velocimetry." Experiments in Fluids **29**(7): S166-S174.

Santiago, J. G., S. T. Wereley, et al. (1998). "A particle image velocimetry system for microfluidics." Experiments in Fluids **25**(4): 316-319.

CHAPTER TWO: DESIGN, FABRICATION AND CHARACTERIZATION OF AN IN-PLANE PASSIVE MICROMIXER

Introduction

Microfluidics is an enabling technology that allows fluids to be processed in smaller volumes and on faster time scales (Floyd-Smith, Golden et al. 2006). Microfluidic channels need much smaller volumes of biochemical reactants than analyzers in traditional technology and their performance is more efficient due to their enhanced heat and mass transfer properties. Another advantage is the precise controllability of flow by applying electric fields, pressure gradient, geometry design of the channel or by a combination of these methods (Niu and Lee 2003). Microfluidic devices are mainly targeted towards chemical and biological applications where rapid and efficient mixing is essential. Mixing is of considerable importance to realizing lab-on-a-chip (LOC) bio-analysis systems since a majority of the applications often involve reactions that require quick and efficient mixing of reactants for initiation (Liu, Stremler et al. 2000). Nevertheless, mixing is greatly limited at the microscale where fluid flow is almost in all cases laminar. In laminar flows, layers of fluid co-flow and slide over their neighboring layers in a parallel manner without significant motion in the transverse direction.

The generic transport equation of any scalar φ (temperature in heat transfer, velocity in momentum and concentration in mass transfer) is given as follows:

$$\frac{\partial \rho\varphi}{\partial t} + \nabla.(\rho\vec{u}\varphi) = \nabla.(\Gamma\nabla\varphi) + S_{\varphi} \quad \textbf{4}$$

ρ, u and Γ are the density, velocity and diffusion constant respectively and S_{φ} is the source term. In a steady state situation with no sink or source terms, the transport phenomenon is governed by diffusion-based and convective-based effects represented by

the first term on the right hand side and second term on the left hand side of the equation respectively.

Flow in microdevices is usually characterized by low Reynolds numbers ($Re = \rho Vd/\mu = 0.01 – 10$) because the inertial effects are very small compared to viscosity related ones. (ρ, V and μ are density, average velocity, and viscosity of the fluid and d is a characteristic length of the system). Therefore, transport processes at the microscale are mainly due to the random motion of the molecules, i. e., diffusion-based processes. Accordingly, the dominating process in micromixing (mass transport) is also based on molecular diffusion, which is relatively slow. Furthermore, values of the Peclet number are relatively high in microchannels ($Pe = Vd/D_{mol} > 100$, where *Dmol*, is the molecular diffusivity), indicating that diffusive mixing occurs at slower rates compared to the timescales associated with fluid motion (Sudarsan and Ugaz 2006). The diffusive mass-flux across an interface of miscible media is proportional to the interfacial area and concentration gradient between the two. Since both the linear proportionality factor of diffusion (the diffusion constant, D_{mol}) and the concentration gradient are constants in most cases, one strategy to enhance the mixing is to maximize interfacial surfaces between the fluids. However, the maximum possible interfacial area generation is related to the viscous dissipation. Thus, efficient mixing and viscous dissipation, i.e., energy consumption, are inevitably interlinked (Hessel, Löwe et al. 2005).

In the low Reynolds number, common methods of mixing used at the macroscale based on inertial or convective processes, such as creating chaotic and turbulent motion, in order to promote mixing, are less likely to be effective. However, some researchers have proposed solutions using inertial effects. Liu et al. proposed an alternative approach to

induce chaotic advections to perturb the lamellae of fluid and increase mixing (Liu, Stremler et al. 2000) . This is achieved by different means such as development of secondary flows inherent to 3D flow geometries. Although the key advantage of the chaotic-advection based strategies is that an exponential rate of mixing is achieved, as opposed to an algebraic rate (e.g. t^{-1}), the structure becomes geometrically complex (Bottausci, Cardonne et al. 2006).

In order to overcome viscous opposition to fluid flow, energy is required to flow the fluid. Micromixers are categorized based on how this energy is provided to the device. The mixing relies either on the pumping energy or provision of other external energy to achieve mixing, termed as passive and active mixing, respectively. Compared with active mixers, passive mixers have the advantages of low cost, ease of fabrication and integration within microfluidic systems and no complex control units being involved since there are no moving parts; in addition passive mixers do not need additional power input. Therefore, passive mixers and typical microstructured flow mixing designs are favorable for single-use disposable units in biological and chemical microsystems. (Hong, Choi et al. 2004). Hessel et al (Hessel, Löwe et al. 2005) published a comprehensive review in which different concepts and designs of micromixers are explained. Serpentine Structure (Liu, Stremler et al. 2000), Modified Tesla Structure (Hong, Choi et al. 2004), Split and Recombine Structure (SAR) (Schonfeld, Hessel et al. 2004) and Chaotic Flow Configuration (Stroock, Dertinger et al. 2002) micromixers are examples of passive mixing devices proposed by researchers in recent years. Although the micromixing problem has been studied widely, there still exists technical challenges related to the performance, fabrication and integration of micromixers.

Here, the effect of the laminar velocity profile on the diffusive mixing is studied and a novel and highly efficient yet very simple design of a passive micromixer which takes advantage of variable inter-lamellae interface velocity is proposed. It was found that mixing performance is highly enhanced if diffusion interfaces between miscible streams attain the highest velocity possible throughout the residence time of fluids in the mixer, given the flow rate, critical dimensions and other design constraints. Experimental observations and numerical simulation results are provided to support the solution proposed to enhance passive micromixing. Based on the idea presented, a 2-D in plane passive micromixer was designed, fabricated and its functionality tested. Furthermore, the idea of achieving variable velocity profile in laminar flow of the proposed mixing scheme is confirmed with the aid of micro Particle Image Velocimetry (μPIV).

Methods and Materials

Theory

In order to explain the micromixing strategy, a simplified theoretical model of the problem is introduced. Consider a film of liquid B, with a given (parabolic) velocity profile, where species A diffuses in from a constant-concentration source (Figure 12). This is a simplifying assumption and actually when two streams inter-diffuse, concentration of species vary but are conserved quantities along the mixing path. The mass diffusion of A inside B is a classic mass transfer problem (Bird, Stewart et al. 2007). It is assumed that diffusion of species would not alter the hydrodynamics of the laminar flow (the viscosity and velocity profile). Another restriction imposed on the problem is that, diffusion takes place slow enough that the diffused species would not penetrate very far into the liquid.

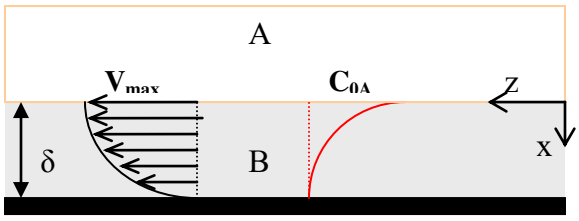

Figure 12 Diffusion of species A into liquid film B; C_{0A} is the solubility limit of A in to liquid B

The velocity profile has a general form of:

$$v_z = v_{\max}[1-(x/\delta)^2] \quad (5)$$

where, x=0 is at the interface, v_z, v_{max}, δ are velocity, maximum velocity and film thickness respectively. Using the transport for diffusion of species A, and considering the fact that mass transfer is predominantly diffusion based in the transverse direction, x (convective term neglected in x) and convection based in the motion direction, z (diffusive term neglected in z), the governing differential equation for concentration distribution of species A, c_A is given as follows with $D_{A,B}$ as the binary diffusion constant:

$$v_z \frac{\partial c_A}{\partial z} = D_{A,B} \frac{\partial^2 c_A}{\partial x^2} \quad (6)$$

Substitution of Eq. (5) in Eq. (6) gives

$$v_{\max}[1-(x/\delta)^2]\frac{\partial c_A}{\partial z} = D_{A,B} \frac{\partial^2 c_A}{\partial x^2} \quad (7)$$

With the following boundary conditions:

z=0 $c_A=0$

x=0 $c_A=c_{A0}$

x=δ $\partial c/\partial x=0$

The solution to this problem is in the form of a series given by P.L. Pigford (1941); however, a limiting expression for small values of δ/v_{max} is given.

Considering the restriction set before, that species A does not penetrate a long distance compared to the thickness of the liquid film, one can argue that species A would observe the liquid film B, to be moving in z direction with a velocity equal to v_{max}. In other words, since A diffuses to a depth very close to the interface, it does not sense the presence of the solid wall at x=δ, hence the variations of the velocity from the interface into depth and towards the wall. Based on this restriction, the current problem can be approximated as a problem of diffusion of A into an infinite thickness layer of liquid moving with the velocity v_{max}. Then, the simplified governing equation becomes:

$$v_{\max}\frac{\partial c_A}{\partial z} = D_{A,B}\frac{\partial^2 c_A}{\partial x^2} \qquad 8$$

By using a similarity variable approach, the solution has the following form:

$$\frac{c_A}{c_{A0}} = 1 - \frac{2}{\sqrt{\pi}}\int_0^{x/\sqrt{4D_{A,B}z/v_{\max}}} \exp(-\xi^2)d\xi = erfc\left(\frac{x}{\sqrt{4D_{A.B}z/v_{\max}}}\right) \qquad 9$$

Once the concentration gradients are known, the local mass flux at the interface may be found as follows:

$$N_{A,x,\text{interface}}(z) = -D_{A,B}\frac{\partial c_A}{\partial x}_{x=0} = c_{A0}\sqrt{\frac{D_{A,B}v_{\max}}{\pi z}} \qquad 10$$

It is observed that if the mass flux - diffusion of species A into B - is to be increased, then one way is to have the highest possible value of v_{max} at the interface of the two miscible fluids since it appears in the numerator of the flux term and increase in v_{max} will lead to increase in the mass flux at the interface. This relationship is a key point for the design of the proposed micromixer.

Looking into the original mixing problem in a micromixer where two streams of miscible liquids, A and B, flowing side by side in a laminar regime in a microchannel, there would be two diffusion fronts developed which progress in the transverse direction of the flow

as one proceeds from the beginning to the end of the channel. It is expected based on the above mentioned, if velocities at the interfaces of the two fluids were increased, the diffusive flux would increase. However, as the two fluids mix, the interfaces would shift away from the centerline as one moves downstream of the channel, i.e., in the increasing z-direction (Figure 13).

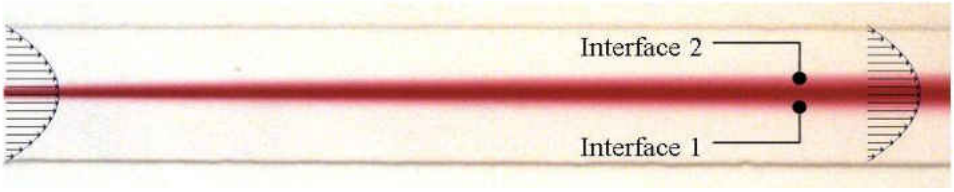

Figure 13 Progression of diffusion interfaces in the transverse direction to the flow; two interfaces are developed and move away from the centerline of the channel as one moves downstream

Based on Einstein's relationship for Brownian motion, it can be shown that the position of the diffusion interface of each of the species (fronts) would progress from the initial location (centerline) in the x-direction (in both ways) as follows:

$$x'(z) = (2D_{A,B}\tau)^{1/2} = (2D_{A,B} \cdot z/U)^{1/2} \qquad 11$$

x, τ and $\bar{U}$ are, displacement of interface from centerline, channel residence time and average fluid velocity respectively.

The two key facts of this work are established as follows:

(1) Mass flux at the interface of species diffusing into a liquid film from a constant source increases as interface-velocity is increased;

(2) Interfaces progress in the transverse direction(x) as we go downstream the channel,

Based on these two facts, novel passive mixer design is proposed that takes advantage of flow profile variation. The sidewalls cause the flow profile to change in such a way that the maximum (v_{max}) is not always in the center line and gets shifted periodically across

the transverse direction. Due to the repeating patterns the shift in maximum velocity occurs periodically where the progressing diffusion fronts and the maximum velocity coincide repeatedly during the residence time of the fluid inside the mixing channel. This is in contrast to the conventional T mixer that has a constant parabolic velocity profile, where the maximum occurs only at the centerline (Figure 13). With respect to the established facts, coincidence of diffusion interfaces with fast moving layers of fluid result in better mass transfer, hence better diffusive mixing. It should be noted that in a microchannel the velocity profile is also dependent on the depth of channel, y coordinate, where as here a 2D configuration was assumed for the velocity that is independent of y; this would not hurt the argument, since it can be said that the result is true at any given y (depth in the microchannel). Velocity, v_z-, would vary along x in the form of a parabolic profile but with different magnitudes depending on y. Detailed study of the effect of the velocity profile and the near wall effects has been performed by Kamholz (Kamholz and Yager 2001) and Ismagilov (Ismagilov, Stroock et al. 2000) where a so called *Butterfly effect* has been detected and explained at the cross-section of microchannel with binary diffusion taking place.

In summary, altering the velocity profile repeatedly throughout the mixing channel of the micromixer tends to increase the mixing performance. The next step is to develop the desired velocity profile which would have its maximum value vary across the transverse direction, x, as a function of the motion wise coordinate, z in a passive manner. This has been accomplished by the design of the sidewalls. In this way not only the maximum of the velocity profile shifts in the transverse direction periodically throughout the channel but also, the overall interfacial area between the two streams is increased which also has a

positive effect on the mixing performance. Each layer of fluid undergoes acceleration and deceleration passing through the mixer and the maximum velocities coincides with the progressing diffusion fronts more often on average and with regards to the established key points developed in this study, diffusive mass flux increases across these interfaces, hence increasing the mixing efficiency of the micromixer. Schematic of the sidewall profile and how the velocity profile is affected passively is illustrated in (Figure 14).

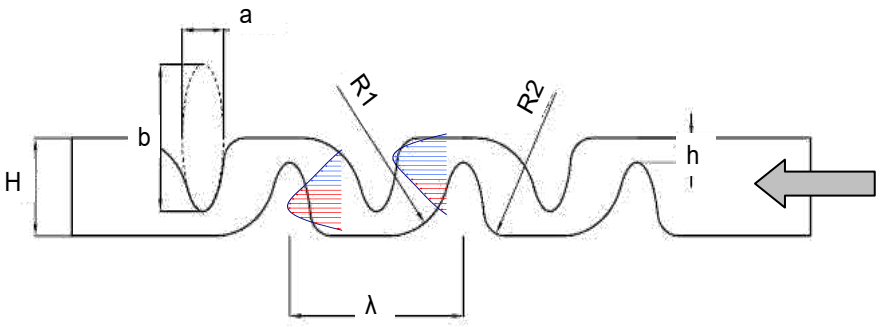

Figure 14 Velocity profile, unlike in a T-mixer, varies throughout the channel passively and periodically due to the sidewall design; sidewall profiles expand and contract asymmetrically (descending slope is steeper than the ascending slope). The velocity profile maximum, shifts transversely such that it coincides with the diffusion interfaces repeatedly. Increased velocity at interfaces, results in enhance flux of species.

Alternating *acceleration and deceleration* of the layers relative to each other lead to high mixing efficiency without resorting to complex features that create stagnation or recirculation of the fluid which leads to trap zones and dead volumes. As shown in (Figure 14), parameters *a* and *b* define the ellipsoid used to generate the side wall patterns. They are chosen such that, asymmetric sidewalls are generated with least parallelism and that the maximum variation of the velocity profile is achieved passively. λ is the periodic length of the repeating sidewall profiles. *H* is predefined as channel width and *h* is the constriction width that together with other parameters makes the sidewalls expand or contract asymmetrically; if chosen too small, then large pressure

drops would occur. Sharp corners are removed by making the walls smooth to ensure that no dead volumes are created in the device (*R*). Numerical simulations resulted in optimized values of *H=200, h=50, a=300, b=100, R=100 λ=400* and with channel depth of 100 (unit: micrometer).

Numerical Simulation

Numerical simulation results are presented to show the effect of velocity profile variation on promoting the diffusive mixing. Velocity profiles extracted at two corresponding cross-sections are shown in (Figure 15) shows the change in velocity profile and the shifting of the maximum from the center towards the side walls from upstream to downstream of the channel in a repeating cell. This shift takes place periodically throughout the channel; hence the interface layers experience a variable velocity in contrast to the case of a straight channel with fixed velocity profile.

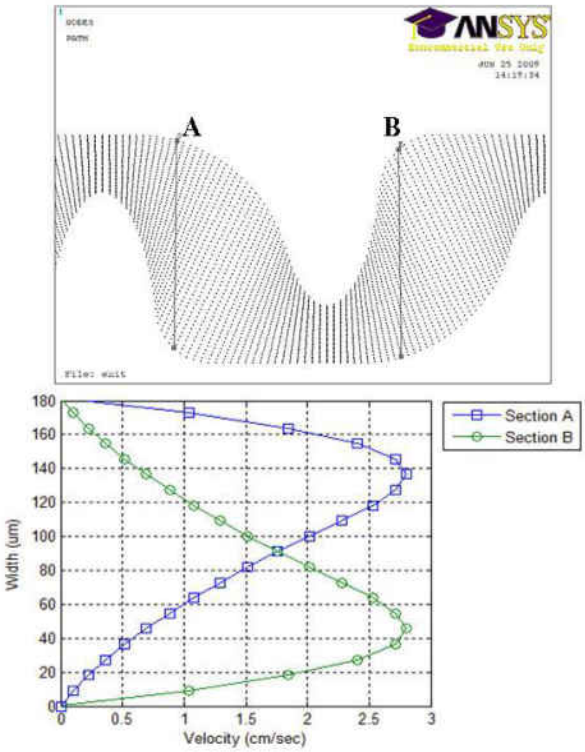

Figure 15 Velocity profiles at A and B resulting from numerical simulations; top layers of fluid move faster than the bottom layers at section A whereas the situation is reversed at section B and the velocity profile maximum shifts across the width of the channel.

The velocity profile variation is achieved by designing the sidewalls in such way that the profiles on the walls are non-symmetric with respect to the centerline of the channel. The upper and lower wall profiles are however repeated periodically with a phase lead or lag. The profiles can be generated using "spline" or "cosine" functions or a combination of circular and ellipsoidal arcs.

In order to evaluate and quantify the mixing performance of the mixer based on the periodic velocity profile variation strategy, a sample case is presented where two aqueous solutions containing analytes A and B are introduced at the inlet. Figure 16 and Figure 17 show comparisons between the mixing performance of a standard T-mixer and the proposed sigma mixer. Load and boundary conditions for the numerical model, e.g. flow

rate, inlet concentration profiles and outlet pressure are chosen such that the governing parameters like the Reynolds (UD_H/ν) and Peclet number ($UD_H/D_{A,B}$) are identical in order for the results to be comparable. The hydraulic diameter is taken to be similar too. (D_H=4A/P where A and P are the inlet cross section area and the wetted perimeter of the channels respectively, U is the average velocity and ν is the kinematic viscosity of the solution). Results are given for a case where Reynolds and Peclet number are 1.65 and 730 respectively. The ideal situation is to have an even distribution of both analyte concentration over the cross-section of the outlet (both analytes having a constant concentration across the width, in this case C* of 0.5). The mixing efficiency is defined as follows:

$$\sigma = [\frac{1}{N}\sum_{j=1}^{N}(c_j - c^*)^2]^{1/2} \quad \textbf{12}$$

c_j is the concentration of cross section nodes and j is the index; The mixing efficiency (%) is defined as :

$$M\% = (0.5 - \sigma) \times 100\% \quad \textbf{13}$$

σ has the form of standard deviation; standard deviation (STD) of the concentration distribution of each analyte over the channel width can be calculated and used as a measure of mixing performance. The lower the deviation from the average value, the better mixing has occurred. Perfect mixing is when the STD goes to zero and an average concentration of C*=0.5 is achieved all over the cross section. As can be seen in (Figure 17) both mixers show similar decrease in mixing performance with increased average flow speed, confirming diffusion dominated mixing mechanism in the highly laminar regime; however, the modified sigma micromixer show superior mixing performance at a given working flow rate.

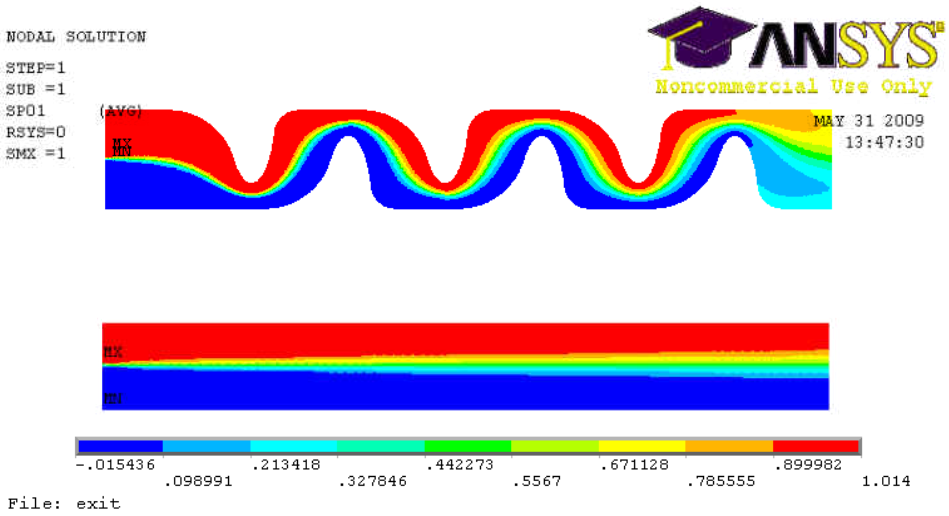

Figure 16 Contour plots of concentration comparing mixing performance of the standard T mixer and the Modified Sigma micromixer. Ideally, at the exit all cross section elements should attain a relative concentration of C*=0.5 showing perfect dispersion of one species in another.

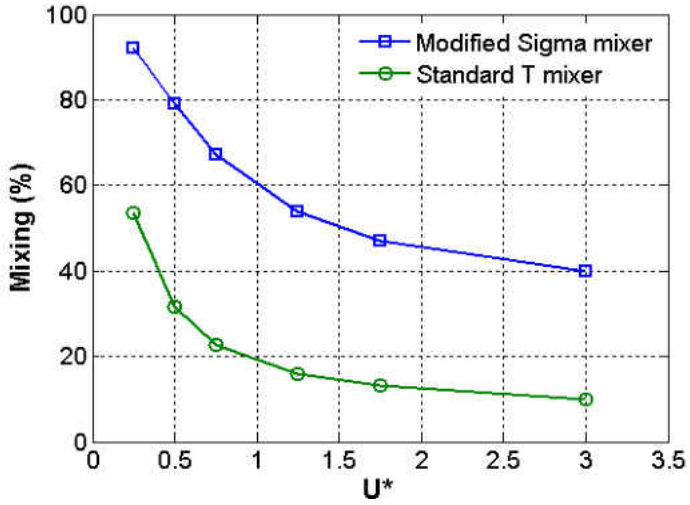

Figure 17 Mixing performance deteriorates for mixers as inlet velocity increases confirming the diffusion-based nature of mixing in microdevices ($U^*=U_{max\_inlet}$ / $[\mu/\rho.D_h]$ ~ Re_{max}, μ=0.001Pa.sec, ρ=1000kg.m^{-3} and D_h=100µm)

In conclusion, numerical results supported the idea that the higher the velocity profile variation is along the mixer length, the better the mixing performance would be. In addition to numerical results, the variation of laminar velocity profile was confirmed using micro Particle Image Velocimetry technique (Figure 18).

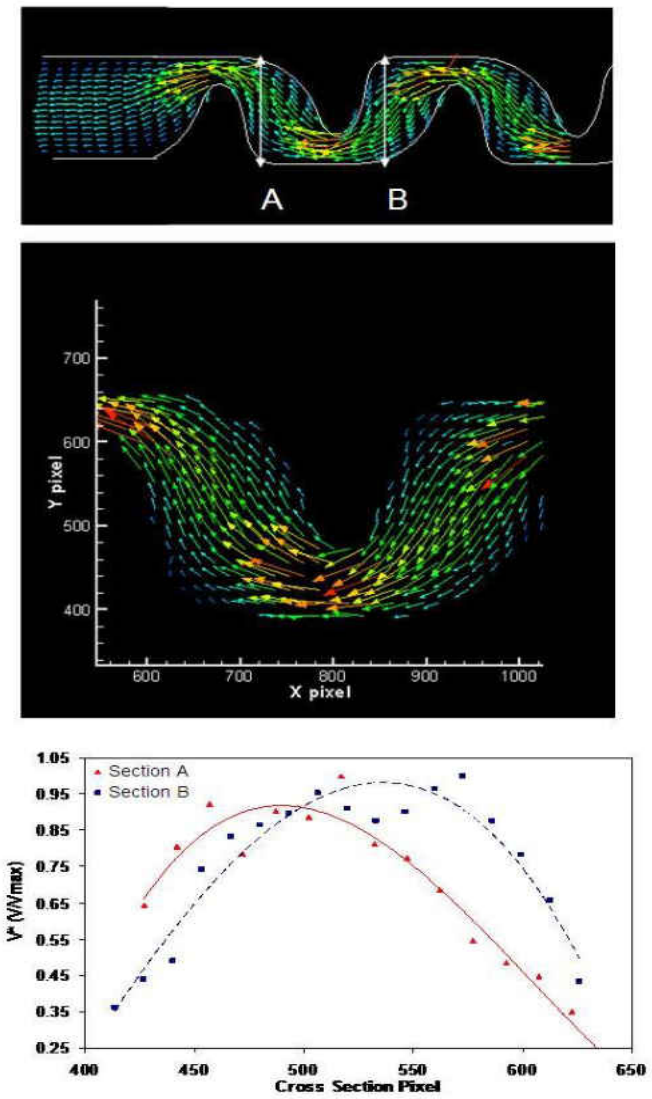

Figure 18 Actual µPIV flow visualization inside the micromixer; top layers at section A move slower than the bottom layers of the fluid where as the situation is reversed in section B. (note the shifting of the velocity profile maximum across the width from A to B)

Fabrication

The proposed micromixer has a 2-D in-plane structure which makes the fabrication and integration convenient. Mixing is achieved without resorting to any complex geometry unlike devices proposed in other designs (Liu, Stremler et al. 2000; Stroock, Dertinger et al. 2002; Jen, Wu et al. 2003; Schonfeld, Hessel et al. 2004). Considering the applications, which can range from one-time use disposable assay chips to integrated

microfluidic platforms for combinatorial chemistry testing devices used in pharmaceutical research, emphasis has been placed on having the simplest yet effective structures of all. In addition, unlike active micromixers, where an external source of energy is required to promote the mixing, the proposed design falls into the category of passive devices which can easily be integrated into any microscale platform and function on a stand alone basis.

A typical procedure of fabricating a microchannel is to spin coat a layer photoresist on a substrate; the thickness of the coating would determine the height of the microchannels. Patterning the photoresist via photolithography is used to make a mold which will eventually be used to replicate channels in an elastomer (Poly-dimethyl-siloxane PDMS). The elastomer which comes in liquid form is mixed with a curing agent and poured on mold and allowed to cure. The PDMS layer consisting of transferred patternes (microchannels) is bonded to another blank layer of PDMS or glass slide to create a closed fluidic channel by surface treatment. Inlet and outlet ports would be punched in the blank layers (Figure 19).

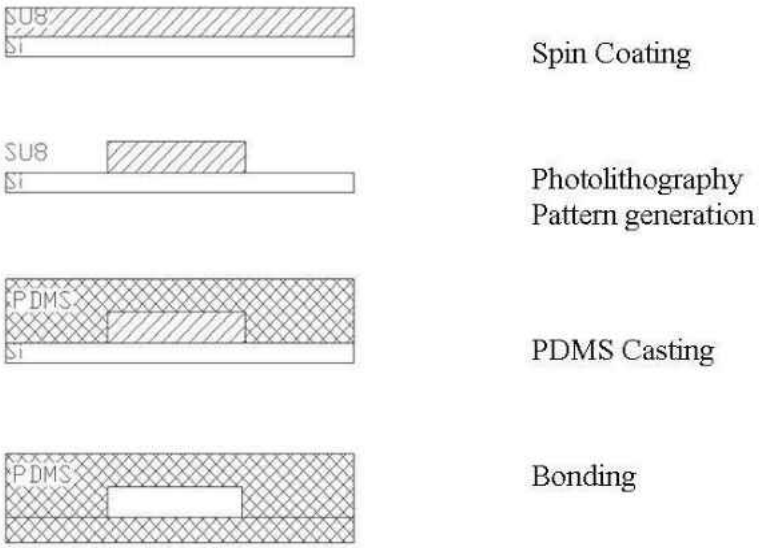

Figure 19 General procedure for making microchannel using the SU8 resist and PDMS replication

SU-8 is a high-contrast, epoxy based negative photoresist used for micromachining and other microelectronic and microfluidic applications, where thick, chemically and thermally stable features are desired. Film thicknesses in the range 0.5 to less than 200 micrometers can be achieved with a single coat process. The exposed and subsequently thermally cross-linked portions of the film are rendered insoluble to liquid developers (Appendix 1). SU-8 is used to create high aspect ratio structures with near vertical walls in very thick films due to its optical properties. In (Figure 20), scanning electron microscopy image of the fabricated devices is shown.

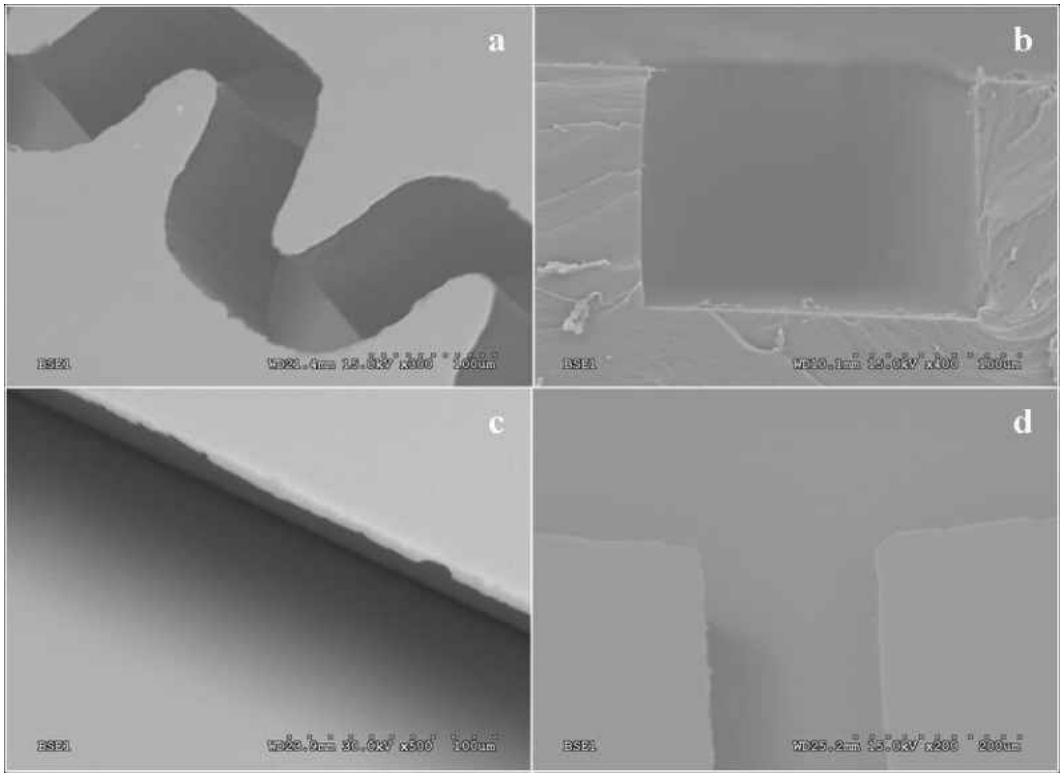

Figure 20 Scanning Electron Microscopy (SEM) images of a) oblique view of the micromixer channel, b) rectangular cross-section of the channel c) smooth surface of the micromixng walls d) intersection of channel with the reservoir

Results - Characterization

In order to observe the efficiency of the proposed micromixer, an accepted method proposed for mixing evaluation is adopted. An experiment was setup where two streams, a base solution (sodium hydroxide) and a pH indicator solution (phenolphthalein) are pumped into the mixer. Upon mixing the transparent solution will turn into pink/purple color (Liu, Stremler et al. 2000)). Phenolphetalein and sodium hydroxide solution are both colorless but once mixed turn into a dark pink/ purple color.

Phenolphthalein solution (phenolphthalein 1 %, isopropyl alcohol 60 %, water balance) and 0.4N sodium hydroxide solution (1.6 % sodium hydroxide in a similar solution to above and pH=12.5) were used. The two colorless solutions are introduced at the inlets of

the devices by an infusion pump. When mixed, a pink/purple region is created which expands transversely with two interfaces away from the centerline as the solutions further mix downstream. Color images (Lee, Kim et al. 2006) at select cross sections are converted into gray-scale images. Pixels with gray intensity I=0, show fully mixed regions whereas bright pixels, I=1, are non-mixed portions of the flow (Figure 21). The deviation of gray intensity around the darkest gray pixel (completely mixed region in the middle of the channel) is calculated for the pixels of the selected cross section (Stroock, Dertinger et al. 2002).

$$\sigma = [\frac{1}{n}\sum_{i-1}^{n}(I_{\min} - I_i)^2]^{1/2} \quad \textbf{14}$$

n is the number of the cross section pixels, *Ii* is gray intensity of pixel *i* of the selected cross section and *Imin* is the minimum gray intensity. When there is no mixing, the standard deviation, σ=1, and ideally at full mixing it will reach 0 as all pixels attain uniform gray intensity (Appendix 2).

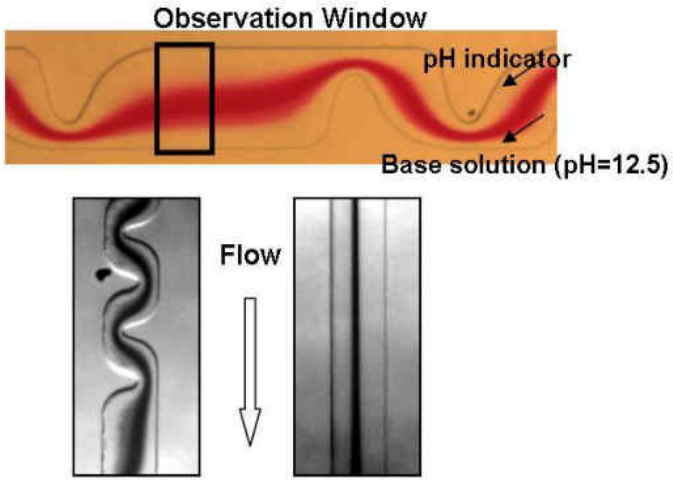

Figure 21 Evaluation of mixing performance using color changes as a result of mixing of a pH indicator (phenolphthalein) and a base solution (sodium hydroxide, pH=12.5) Performance of Modified Sigma and the Standard T mixers at 3mm mixing length; the wider the gray region, the better the solutions have mixed(Re=0.4, Q=350µl.hr^{-1}, $D_{hydraulic}$ = 66µm)

The level of mixing (percentage) is defined as follows:

$$M(\%) = (1-\sigma) \times 100 \quad (15)$$

The mixing performance was evaluated in comparison to the T mixer and the Modified Tesla Structure mixer as a function flow Reynolds number and mixing length (Figure 22). The result validates the effectiveness of the proposed passive micromixing concept and improvement of mixing performance. In addition to having the advantage of no-dead volume, the sigma mixer achieves satisfactory mixing in smaller mixing lengths; hence favorable option for limited size chips and platforms.

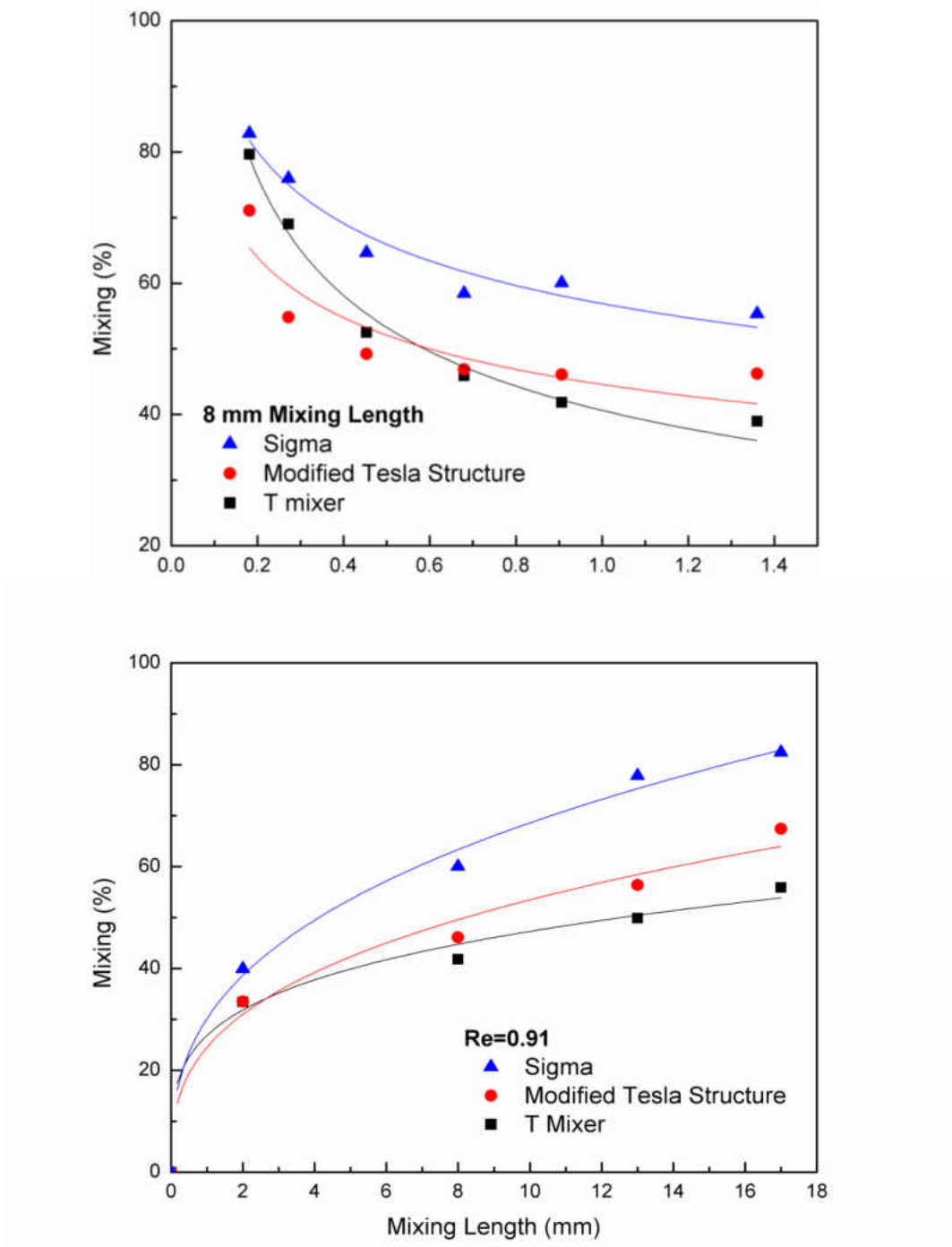

Figure 22 Mixing performance at a given mixing length (L=8 mm) as a function of flow Reynolds number, b) Mixing performance at a given flow rate (Q=1000 µl/hr, Re=0.91) as a function of mixing length.

Conclusion

In this study, it was demonstrated that the diffusive mass flux between streams of fluid flowing in a laminar regime increases as the velocity of the interface between the streams of liquid increases; Since, the interfaces progress in the transverse direction as one moves downstream the flow, by causing the maximum of the velocity profile to be shifted from the centerline to coincide with the moving interfaces as often as possible, significant improvement in mixing can be expected. A novel micromixer concept has been proposed based on this idea. Numerical simulation was performed and based on the results, a 2-D in-plane micromixer was fabricated and its functionality verified by color analysis due to mixing of phenophetalein (pH indicator) and sodium hydroxide (pH=12). The proposed micromixer can be adopted to a wide-range of microfluidic applications in the low Reynolds number flows. The simple yet effective design facilitates the fabrication and integration of the proposed micromixer which is favorable for disposable polymer-based biochemical assay chips. The micromixer is passive thus energy efficient and is expected to be compatible with various pumping mechanisms including capillary, hydraulic, and electrokinetic systems. Finally, the device has no dead volumes or recirculation zones, causing otherwise incomplete homogenization or cross-contamination of reagents. The proposed device can be fabricated and integrated with a single mask photolithography very easily due to its in-plane structure, making it superior and more favorable for mass produced disposable micro-fluidic platforms.

List of References

Bird, R. B., W. E. Stewart, et al. (2007). Transpot Phenomenon. New York, J. Wiley.

Bottausci, F., C. Cardonne, et al. (2006). "An Actively Controlled Micromixer: 3-D Aspect." Microfluidics: History, Theory and Applications.

Floyd-Smith, T. M., J. P. Golden, et al. (2006). "Characterization of passive microfluidic mixers fabricated using soft lithography." Microfluid Nanofluid **2**: 180-183.

Hessel, V., H. Löwe, et al. (2005). "Micromixers—a review on passive and active mixing principles." Chemical Engineering Science **60**: 2479-2501.

Hong, C.-C., J.-W. Choi, et al. (2004). "A novel in-plane passive microfluidic mixer with modified Tesla structures." Lab Chip **4**: 109-113.

Hong, C. C., J. W. Choi, et al. (2004). "A novel in-plane passive microfluidic mixer with modified Tesla structures." Lab Chip **4**: 109-113.

Ismagilov, R. F., A. D. Stroock, et al. (2000). "Experimental and theoretical scaling laws for transverse diffusive broadening in two-phase laminar flows in microchannels." Applied Physics Letters **76**(17): 2376-2378.

Jen, C. P., C. Y. Wu, et al. (2003). "Design and simulation of the micromixer with chaotic advection in twisted microchannels." Lab Chip **3**: 77-81.

Kamholz, A. E. and P. Yager (2001). "Theoretical analysis of molecular diffusion in pressure-driven laminar flow in microfluidic channels." Biophysical Journal **80**: 155-160.

Lee, S. W., D. S. Kim, et al. (2006). "A split and recombination micromixer fabricated in a PDMS three-dimensional structure." Journal of Micromechanics and Microengineering **16**(5): 1067-1072.

Liu, R. H., M. A. Stremler, et al. (2000). "Passive Mixing in a Three-Dimensional Serpentine Microchannel." Journal of Microelectromechanical Systems **9**: 190-197.

Niu, X. and Y.-K. Lee (2003). "Efficient spatial-temporal chaotic mixing in microchannels." Journal of Micromechanics and Microengineering(13): 454-462.

Schonfeld, F., V. Hessel, et al. (2004). "An optimised split-and-recombine micro-mixer with uniform chaotic mixing." Lab Chip **4**: 65-69.

Stroock, A. D., S. K. W. Dertinger, et al. (2002). "Chaotic Mixer for Microchannels." Science **295**(25): 647-651.

Stroock, A. D., S. K. W. Dertinger, et al. (2002). "Chaotic Mixer for Microchannels." Science **295**(5555): 647-651.

Sudarsan, A. P. and V. M. Ugaz (2006). "Fluid mixing in planar spiral microchannels." Lab on a Chip **74**(6): 74-82.

APPENDIX A: SU-8 & PDMS PROCESSING – MICROFLUIDIC CHANNEL FABRICATION

A typical procedure of fabricating a microchannel is to spin coat a layer photoresist on a substrate; the thickness of the coating would determine the height of the microchannels. Patterning the photoresist via photolithography is used to make a mold which will eventually be used to replicate channels in an elastomer (Poly-dimethyl-siloxane PDMS). The elastomer which comes in liquid form is mixed with a curing agent and poured on mold and allowed to cure. The PDMS layer consisting of transferred patternes (microchannels) is bonded to another blank layer of PDMS or glass slide to create a closed fluidic channel by surface treatment. Inlet and outlet ports would be punched in the blank layers.

SU-8 is a high-contrast, epoxy based negative photoresist used for micromachining and other microelectronic and microfluidic applications, where thick, chemically and thermally stable features are desired. Film thicknesses in the range 0.5 to less than 200 micrometers can be achieved with a single coat process. The exposed and subsequently thermally cross-linked portions of the film are rendered insoluble to liquid developers. SU-8 is used to create high aspect ratio structures with near vertical walls in very thick films due to its optical properties.

Substrate Preparation

Silicon wafers (mechanical grade) are usually used as base substrates; although other polished substrates can be used as well. Surface of the substrate needs to be clean, since the adhesion of SU-8 coating to the substrate is adversely affected by surface contaminations. Clean the wafer using basic cleaning methods. (For best results,

substrates should be cleaned with a piranha wet etch using H_2SO_4 and H_2O_2 followed by DI water rinse). Blow-dry the wafers. After cleaning, place the wafers on 100°C hotplate for 5 minutes for dehydration.

Coating

SU-8 resists are available in various standards viscosities (this manual is prepared for SU-8 50 provided by MicroChem®). For a desired coat thickness, depending on the viscosity value, appropriate spin-speed should be chosen based on the graphs and tables provided in manufacturer's specification sheet.

(a) Apply adequate resist on the substrate (4 ml for 3 inch wafers).

(b) Use a two stage spin coat program as follows (for film thickness : 100 – 120 μm) :

- 15 seconds @ 500 rpm, acceleration: 85
- 45 seconds @ 1000 rpm, acceleration: 850

(c) Edge bead removal; the resist accumulates on the edges which needs to be removed using a blade to ensure well-controlled contact with the mask; otherwise vertical side walls will not be achieved.

Soft Bake

A level hotplate with good thermal control and uniformity is recommended over convection ovens. Soft bake is performed in a two stages:

(a) 10 minutes on 70°C hotplate

(b) 30 minutes on 105°C hotplate

Allow the wafer to cool down at room temperature before proceeding on to next steps. In case, wrinkles appear on the surface of the resist, leave the wafer on the hotplate for a

few minutes. Repeat the cool-down and heat-up cycle until wrinkles are no longer seen on the film.

Alignment and Exposure

Follow the instructions given for the EVG aligner to perform the adjustments and exposure (since a single layer mask is used, alignment is not critical as long as the features are in bounds of the wafer). SU-8 is optimized for near UV (350-400nm) exposure. The optimal exposure dose will depend on film thickness (thicker films require higher dosage) and process parameters.

(a) Follow EVG aligner procedures to load mask and wafer.

(b) Expose for 24 seconds (total dosage for targeted thickness is within 350-400 mJ/cm^2)

Adhesion failure, severely negative sidewalls and excessive cracking are often indications of an under cross-linking condition. To correct the problem, increase your exposure dose and or increase your post exposure bake (PEB) time.

Post Exposure Bake (PEB)

PEB should take place directly after exposure. PEB is also a two step baking using hotplates:

(a) 3 minutes on 75°C hotplate

(b) 10 mintues on 105°C hotplate

(c) Allow wafer to cool down to room temperature (thermal shocks will results in form of cracks or peeling off of the coating if the hot wafers are placed in the developing solution) After 1 minute of PEB at the higher temperature, an image of the patterns

should be visible in the SU-8 coating. If no visible latent image is seen during or after PEB this means that there was insufficient exposure, heating or both.

Development

SU-8 developer provided by Microchem® is used for developing the patterns (other solvent based developers such as ethyl lactate and diacentone alcohol may also be used). Developing time vary largely based on agitation and other factors.

(a) Prepare petri dishes containing SU-8 developer and isopropyl alcohol (IPA).

(b) Recommended developing time is 7 – 10 minutes however, developing time may be extended (up to 25 minutes). To find out the completion of the developing process, immerse the wafer into the IPA; if a milky residue is observed then the development is NOT completed yet.

(c) Once clear patterns emerge and no residue is seen, rinse with IPA and blow dry using the nitrogen (air) gun.

There is a low risk of over-developing for SU-8; therefore the developing process can be extended to ensure completion of the process.

Casting – PDMS processing

The fabricated SU-8 mold will be used to replicate patterns in the elastomer resin. Patterns can be replicated as many times, depending on the quality of the mold. Sylgard 184 Silicone® provided by Dow Corning is used for fabricating the microchannels. Conventionally, Sylgard 184 is used for microelectronic packaging applications due its

robustness, stability and reliability, both mechanical as well as electrical properties. The two part resin is processed using the following steps:

(a) Place the processed SU-8 mold in a clean petri-dish and tape the edges to the bottom so it doesn't move.

(b) Place an empty disposable dish on the laboratory scale and zero the scale

(c) Pour appropriate amount of base resin and curing agent in 10:1 proportion; usually, 15 grams of base elastomer is sufficient to cover a 3"wafer and create a semi-rigid layer; to construct a closed microchannel, two layers are needed)

(d) Stir the mixture thoroughly so that the curing agent and elastomer are homogenously mixed.

(e) Pour half of the mixture on the wafer that has been tapped to the bottom of the petri-dish and the remainder in an empty petri dish (to form the blank layer)

(f) Allow the mixture to cure at room temperature. Curing process takes more that 48 hours. Accelerated curing can also be done using the following guidelines; however, unwanted bubbles could be trapped during the accelerated process since curing occurs very fast and there is not enough time for the degassing of the liquid resin.

- 35 minutes @ 100°C or 20 minutes @ 125°C or 10 minutes @ 150°C

Ports – Bonding

Once the PDMS layers (blank layer and layer with patterns) are cured, they can be bonded together to make a closed and leak-free microchannel (Figure 23).

Before bonding, holes are punched in the blank layer using a template. The two surfaces need to be activated such that when they are brought in contact they would stick

permanently. For this purpose, oxygen plasma surface activation can be performed. The surface modification for PDMS is fairly robust and a handheld Corona plasma generator is sufficient for the surface treatment.

(a) Place the layers with bonding surfaces facing upwards on the flat disk shown in (Figure 24). Insert the electrode head in the corona machine and connect the power supply.

(b) Adjust the height such that the electrode head is 1 cm above the surfaces.

(c) Remove the samples to tune the plasma arc; there is a tuning knob on top of the machine which can be used to adjust the arc power. To avoid sparks, remove any metallic objects (rings, watches and mobile phones) away from the electrode head. The appropriate arc develops in the form of a stable blue flame having a buzzing sound. (Too low voltage on the tuning knob does not develop a flame, while excess voltage on the other hand, causes sporadic sparks and destabilization of the flame). Once the tuning is done, turn off the power and replace the samples on the disk to perform the surface treatment.

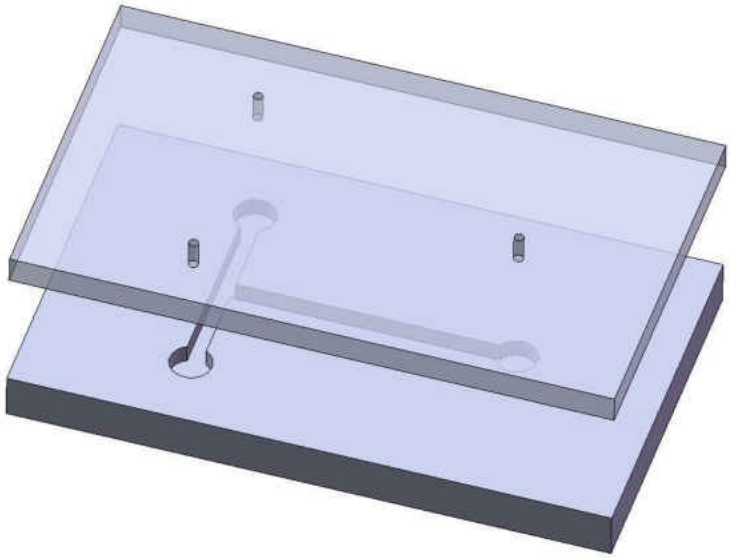

Figure 23 Two layers of PDMS (top: blank - bottom: with patterns) are bonded to form a closed microchannel; inlet and outlet ports are punched in the blank layer prior to bonding

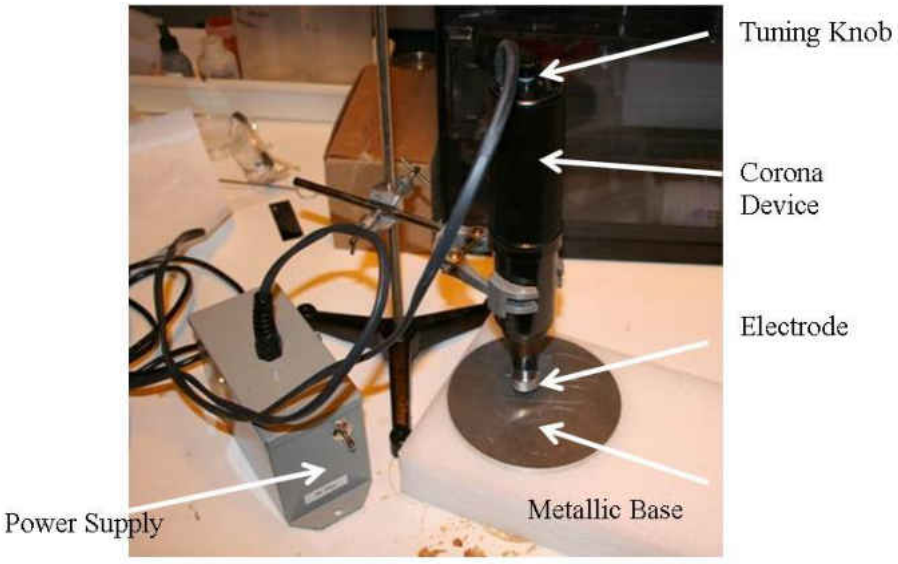

Figure 24 Corona surface treatment machine is used to bond pdms-pdms or pdms-glass layers

(d) Turn on the power supply and slowly sweep the surfaces under the flame for surface activation. Treat the surfaces for approximately one minute each.

After turning off the power, lift the blank layer with a tweezers, minimizing the contacts with the treated surfaces. Align holes on the blank layer with their counter part reservoirs on the pattern layer and gently press the two activated surfaces in contact. Apply gentle pressure on the two layers. Surfaces should be bonded after 5 – 10 minutes.

APPENDIX B: IMAGE PROCESSING

Introduction

Different methods have been proposed for evaluating the performance and optimizing the design of micromixers. A common quantification technique is using dilution of a tracer dye to determine the extent of mixing; for example fluorescent dye and a corresponding microscope with a filter set are required. The intensity image can then be recorded and evaluated. Since the concentration of the dye is proportional to the intensity of the recorded image, the uniformity of the concentration image can be quantified by determining the standard deviation of the pixel intensity values[1] [2]. Another quantification method is measuring the fluorescent product of a chemical reaction occurring due to mixing of two or more reagents introduced to a micromixer [3].

Here we use a characterization method based on color changes resulting from mixing of a pH indicator solution and a base (pH>7) solution. Phenolphthalein solution (phenolphthalein 1 %, isopropyl alcohol 60 %, water balance) and 0.4N sodium hydroxide solution (1.6 % sodium hydroxide in a similar solution to above and pH=12.5) will be used. The two colorless solutions are introduced at the inlets of the devices by an infusion pump. When mixed, a pink/purple region is created which expands transversely with two interfaces away from the centerline as the solutions further mix downstream. Color images at select cross sections are converted into thresholded grayscale images.

[1] Liu R H *et al* 2000

[2] Stroock A D et al 2002

[3] Kamholz A E *et al* 1999

Dark pixels, gray intensity I=0, show fully mixed regions whereas bright pixels, I=1, are non-mixed portions of the flow. Standard deviation of gray intensity around the darkest gray pixel completely mixed region in the middle of the channel) is calculated for the pixels of the selected cross section

$$\sigma = [\frac{1}{n}\sum_{i-1}^{n}(I_{\min} - I_i)^2]^{1/2}$$

n is the number of the cross section pixels, I_i is gray intensity of pixel i of the selected cross section and I_{min} is the minimum gray intensity. When there is no mixing, the standard deviation, σ=1, and ideally at full mixing it will reach 0 as all pixels attain uniform gray intensity. The level of mixing (percentage) is defined as follows:

$$M\% = (1-\sigma)\times 100$$

The mixing performance is as a function of flow Reynolds number, Peclet number and mixing length.

$$\mathrm{Re} = \rho U D_h / \mu$$

$$Pe = LU / Diff$$

ρ: fluid density

U: average fluid velocity

D_h: microchannel hydraulic diameter

μ: fluid viscosity

L: mixing length

Diff: diffusion coefficient of liquids

At a given flow rate (required flowrate), the shorter the mixing length (L), the better is the performance of a micromixer. Similarly, when limited mixing length is allowed, flowrate and channel geometry should be chosen such that appropriate Re and Pe numbers are achieved to ensure mixing.

Setup

Using an infusion pump, the base solution (pH=12.5) and indicator solution are introduced to the inlets of the microchannel. A single outlet will be used to extract the mixed solution out into a beaker. Set the appropriate flow using control keypad on the infusion pump (Figure 25). Since all physical properties are constant, flowrate can be changed to achieve various Re numbers.

The micromixer is placed under a microscope equipped with a color digital camera. The images can be viewed on a computer screen and be saved for image processing.

Figure 25 Infusion pump with control keypad

Image Processing

- Initial correction / enhancement using conventional imaging software such as Microsoft Office Picture Manager.
    - Click *Edit Pictures Tool* → *Color*→ *Enhance Color.* Place the crosshair cursor on a region which is supposed to be clear (white background)
    - Choose an appropriate observation window using: *Edit Pictures Tool*→*Crop.* Crop a window equal to the width of the channel and a length equal to 100 pixels
    - Save the resulting image (Figure 26)

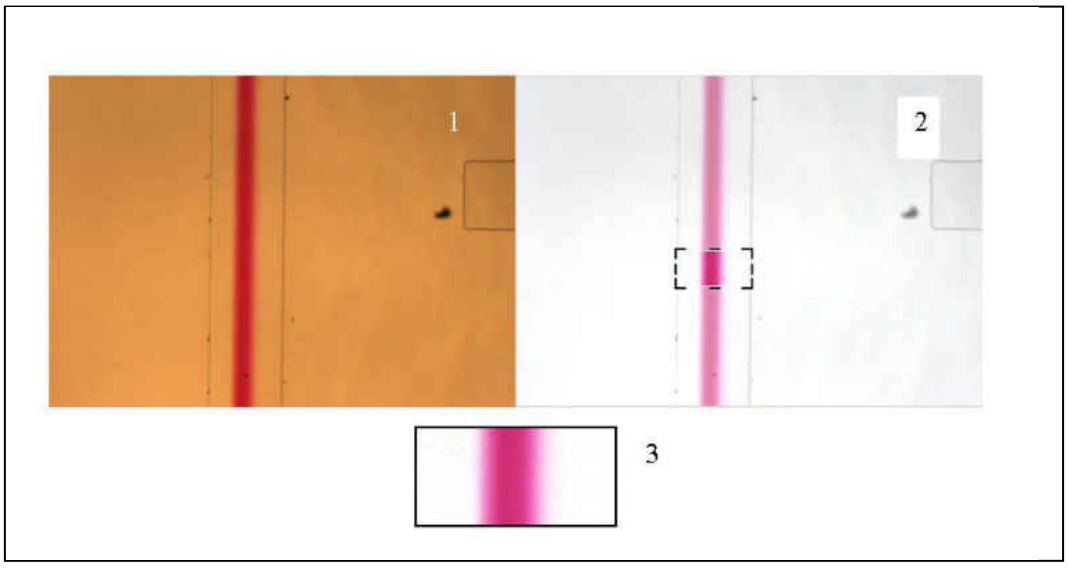

Figure 26 Initial image correction / enhancement

- Read the file from previous step in MATLAB using *imread* command
- Convert the image into grayscale using *rgb2gray* command

- Adjust the grayscale image using *imadjust* command
- Extract the center row of the resulting matrix (Figure 26 -3) and plot the grayscale values of pixels across the channel width.
- Calculate σ and M% using the following formula for data points and plot mixing efficiency (%M) vs Re (flowrate) (Figure 27):
    - $\sigma = [\frac{1}{n}\sum_{i-1}^{n}(I_{\min} - I_i)^2]^{1/2}$
    - $M\% = (1-\sigma)\times 100$

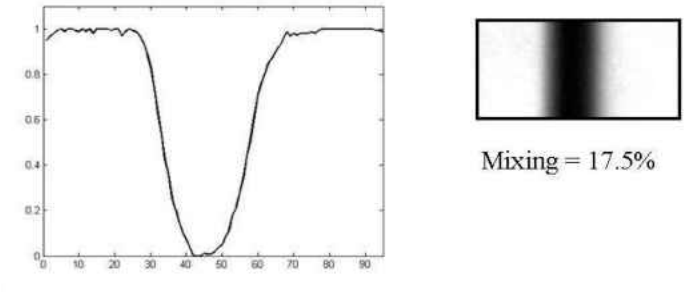

Figure 27 Grayscale intensity across the channel width (Note: black color Imin=0). For ideal mixing all pixel should attain a grayscale intensity of 0 showing the gray band has expanded over the entire channel width

Summary

1. Open microsoft office picture manager

2. Click *edit picture* → crop (on right side of screen) → crop image (note the image size : width pixels x length pixels)

3. Click *edit pictures* → *color* (on right side of the screen) → *enhance color* → place cursor in a region outside the pink area and click

4. Save image

5. read image in matlab : `R=imread('filename.tif');`

6. convert to grayscale : `I= rgb2gray (R);`

7. enhance contrast: `J= imadjust(I);`

8. rescale to range of 0 – 1 : `J= double(J)/255;`

8. see results: `figure, imshow(I), figure, imshow(J),`

9. check the size of enhance image: size(J) → [W x L] should be equal to what to noted in microsoft office picture manager

10. plot the grayscale of a middle column (or row depending on your image orientation) across the width of the channel: `figure, plot(J(:,L/2))`

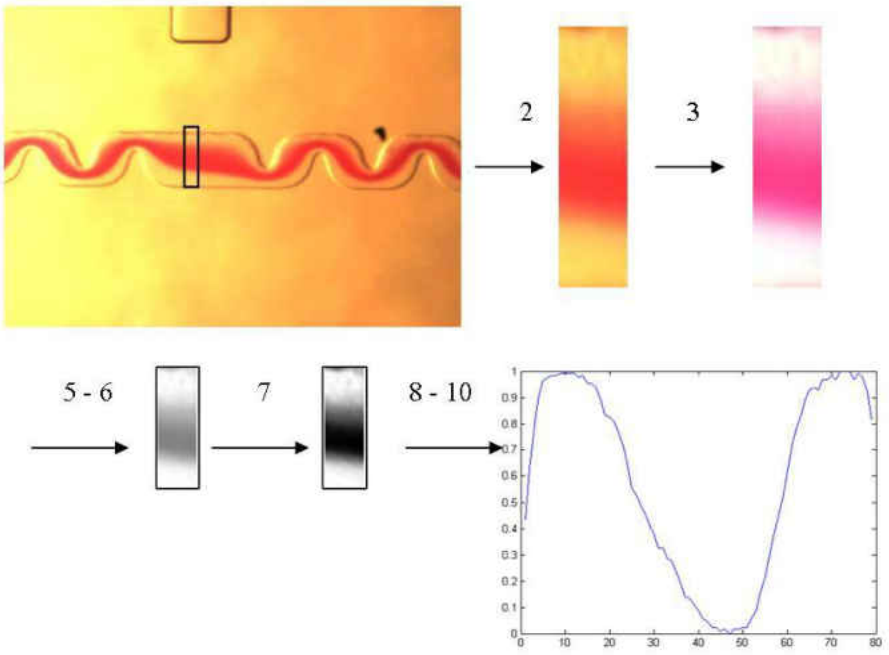

Figure 28 Sequence of steps in image processing for mixing evaluation

11. calculate sigma: $\sigma = [\frac{1}{n}\sum_{i-1}^{n}(I_{\min} - I_i)^2]^{1/2}$ and mixing percentage $M\% = (1-\sigma)\times 100$

For example image size is [79 x 23]:

```
for i=1:79
SUM=SUM+(J(i,12)-MIN).^2;                calculating      the
summation
end
SIGMA=sqrt(SUM/79)        square root
SIGMA = 0.6949
MIXING=(1-SIGMA)x100
```